HOKKAIDO UNIVERSITY

Title	Physical Studies on Deposited Snow. IV. ; Mechanical Properties. (3)
Author(s)	YOSIDA, Zyungo; OURA, Hirobumi; KUROIWA, Daisuke et al.
Citation	Contributions from the Institute of Low Temperature Science, 13, 55-100
Issue Date	1958-06-25
Doc URL	https://hdl.handle.net/2115/20222
Type	departmental bulletin paper
File Information	13_p55-100.pdf

Hokkaido University Collection of Scholarly and Academic Papers : HUSCAP

Physical Studies on Deposited Snow. IV.*
Mechanical Properties (3).

by

Zyungo YOSIDA, Hirobumi OURA, Daisuke KUROIWA,
Tosio HUZIOKA, Kenji KOJIMA and Seiiti KINOSITA
Applied Physics Section, Institute of Low Temperature Science.

(Manuscript Received April 1958)

II. Mechanical Properties of Deposited Snow.

(continued from previous paper)

The Contraction of Snow at Constant Speeds.

§ 15. The contraction of snow mass at constant speeds.

As is well known, the snow cover deposited on the ground subsides gradually. Each of the snow layers composing it undergoes in two or three weeks such a large amount of contraction as to diminish its thickness to about half the original one with no sign of fracture in its structure. The present authors, as shown in Part II of this series of papers (Physical Studies on Deposited Snow), found simple mathematical formulae representing the relationships between the coefficient of compressive viscosity η of snow and its density ρ or the time t. On the other hand, when one tries to compress the snow to its half thickness in a short time, it will without exception be broken down. The present authors reported in Part III of this series of papers their study of the resisting force which the snow exerted against a body dropped upon it. In this case the snow was of course fractured and ruptured by being severely compressed in a very short time by the falling body.

The above described facts indicate obviously that the snow is subjected to different manners of deformation, which may be called destructive or non-destructive, according to whether it is deformed rapidly or slowly although the final amount of the deformation should be the same. Then it will come into question in what way the manner of deformation is altered when the rate of deformation is changed step by step. In order to study this point the present authors made a series of experiments in which the snow was compressed at constant speeds of different magnitudes (*1*). Such compressing experiments have already been performed by some authors (*2*) (*3*) (*4*) (*5*), but they seem to have paid little attention to the above-stated question of the change in the manner of deformation. However their results proved to be

* Contribution No. 392 from the Institute of Low Temperature Science.

very helpful to the present authors in preparing the experiments, especially in predetermining the range of compressing speeds needed for the experiments.

Fig. 1 shows the experimental equipment. S is the pillar of snow to be compressed. It stands on brass plate B which forms the top of a device to measure

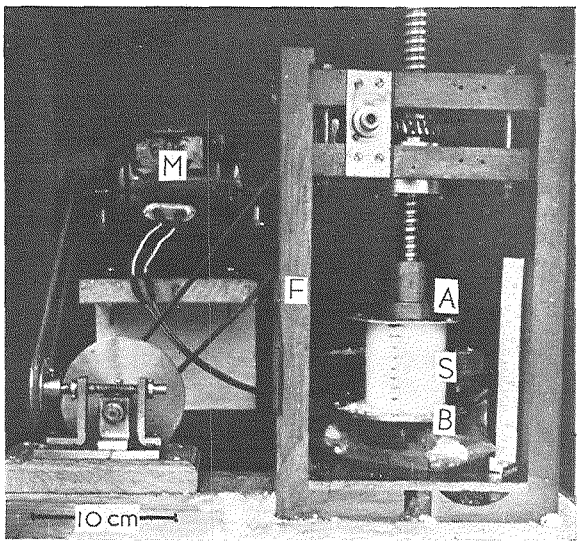

Fig. 1 Experimental equipment for compressing snow at low speeds.

the force applied on it by snow pillar S. Electric motor M pushes down compressing iron block A slowly by means of the reduction gears shown in the figure. The advancing speed of A can be altered in the range from 1 mm/min to 1 m/min by changing the reduction ratios of the gears and the rotating speed of the motor. Frame F is made of cast iron.

The force applied on plate B is the same in magnitude as the force with which the snow pillar is compressed. The device to measure this force is constructed as follows. An iron rod is attached to the bottom of plate B and is supported by two plates of phosphor bronze (not seen in the figure). On their surfaces are cemented strain gauges. When the force acts upon plate B the phosphor bronze plates are slightly bent and the fine wires contained in the strain gauges are made to change their electric resistance in proportion to the magnitude of the force. This change in the electric resistance is registered by a recording galvanometer or by an electromagnetic oscillograph.

All the snow samples used in the following experiments were compact snow of medium density.

§ 16. Visual observation of the manner of contraction of snow. Plastic and destructive contractions.

The series of photographs illustrated in Fig. 2 shows the course of contraction

of a snow pillar when it was compressed at a speed as small as a few millimeters per second. The pillar contracted continuously without fracture. The marks tinted on its surface with powdered rouge displaced in such a way that each of their intervals was lessened nearly at the same ratio; the pillar contracted uniformly along its whole length. The contraction ratios of the intervals observed on one sample of snow are listed in the following table. Except in the intervals Nos. 2,

No. of interval from above	1	2	3	4	5	6	7	8	9	10
Contraction ratio in %	62	78	75	58	58	59	61	52	61	59

Each of the intervals was initially about 1 cm long.

3, 8 the contraction ratio shows nearly the same value of 60%. It is supposed that the exceptions were caused by the existence in these intervals of thin snow layers stronger or weaker than the average snow.

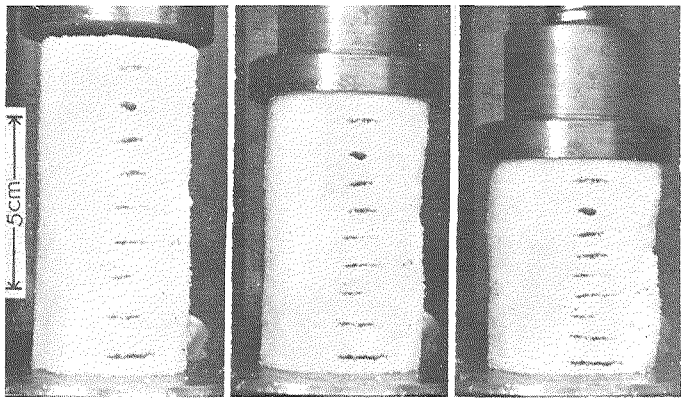

Fig. 2 Plastic contraction of a snow pillar. Compressing speed: 4.8 mm/min. Density of snow: 0.38 gr/cm³. Temperature: −3°C. Diameter and height of the pillar at the beginning of the experiment were 4.6 cm and 10 cm respectively. In the final stage shown in the photograph on the right the resisting force R of snow amounted to 82 kg (4.9 kg/cm²).

When the compressing speed is raised to above ten or twenty millimeters per minute, the snow pillar comes to contract in quite a different way. It contracts not uniformly through the whole length as in the above case but in such a way that it is broken down near its end plane and the broken snow is squeezed out in fragmentary form towards the periphery of the pillar. On the other hand, the remaining portion of the pillar seems to be kept in the same state as in the original. An example of such a way of contraction is illustrated by the photographs of Fig. 3. The lower end of the pillar is broken and the squeezed out snow is piled up around the foot of the pillar. The marks on the surface of the remaining portion

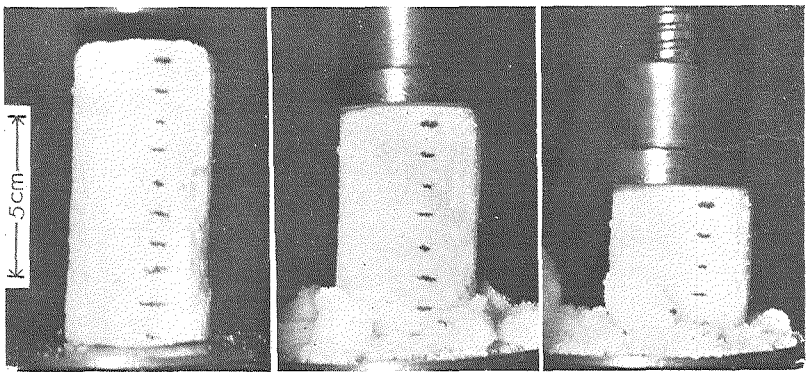

Fig. 3 Destructive contraction of a snow pillar. It was broken down at the plane of its bottom and fragments of snow were piled up around the foot of the pillar. Compressing speed: 24.5 mm/min. Density and temperature of snow: the same as in Fig. 2. Initial diameter and height of the pillar were 4.6 cm and 9.8 cm respectively. The maximum value R^* of the resisting force was 17 kg (1.0 kg/cm^2).

of the pillar keep their intervals unaltered indicating that this portion has undergone little or no contraction. The break-down of the snow does not always occur at the bottom of the pillar; it may occur on the top or on both the top and bottom.

Let the continuous contraction observed in the former case be called *plastic contraction* while that in the latter case caused by the ejection of snow at the end of the pillar be called *destructive contraction.*

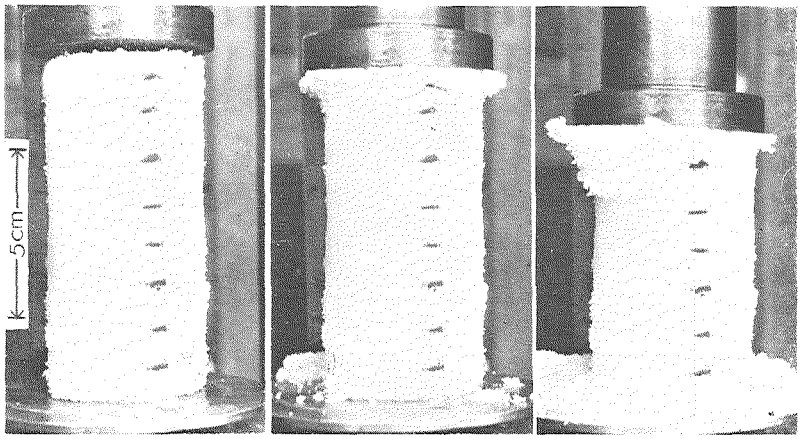

Fig. 4 Destructive contraction of wet snow. The break-down of the pillar occurred at its top and the broken snow was squeezed out in the form of a tongue. Compressing speed: 39 mm/min. Density of snow: 0.39 gr/cm^3. Temperature: 0°C. Initial diameter and height of the pillar were 4.6 cm and 10.4 cm respectively. The maximum value R^* of the resisting force was 9.6 kg (0.58 kg/cm^2).

When the snow pillar is wet and is compressed at speed used in the cases of destructive contraction the snow squeezed out at the end is not fragmented but takes the form of a thin plate hanging from either end like a tongue as shown in Fig. 4. But such a way of squeezing out of snow in the form of thin plate is not restricted to the cases of wet snow: it is observed also on the dry snow of the temperature a few degrees below 0°C when the pillar is compressed at a much higher speed. Some further discussion will be offered on this subject in article (7) of §19 below.

The plastic and destructive contractions manifest themselves in the following manner when the iron compression block (A in Fig. 1) is made to penetrate into the surface of a large block of snow. The photographs of Fig. 5 are spray figures (figures made by spraying coloured water on the surface of snow. See p. 6 of Part III of this series of papers) on the cut surface of the snow block through the center of the depression made on it by the iron compression block. In the case of a low compressing speed (Fig. 5 **a**) the depression on the snow surface takes a

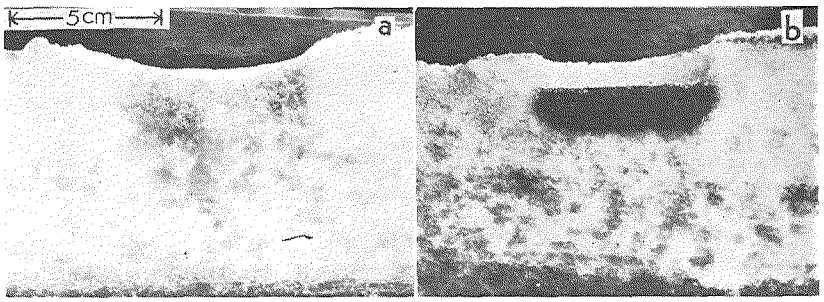

Fig. 5 Spray figure on the cut surface through the centre of the depression made on the upper surface of snow block by the descending iron block. Density of snow: 0.26 gr/cm³. Temperature: −2°C.
a. Plastic contraction. The depression is conical in form. The snow is diffusely tinted. Compressing speed: 2.6 mm/min. The resisting force amounted to 28.5 kg (1.04 kg/cm²).
b. Destructive contraction. The depression takes the form of a hole with vertical wall. The broken snow accumulated below the compressing iron block to form the region of compressed snow which is shown in the photograph by the deep coloration. Compressing speed 5.2 mm/min. Maximum value R^* of the resisting force: 9.4 kg (0.34 kg/cm²).

conical form and the snow is tinted most by the sprayed water just below the depression, the tint diffusing sidewards and downwards with no distinct boundary of the tinted region. Such a diffused coloration indicates that the snow has been subjected to continuous deformation without undergoing any fracture. In the case of high compressing speed the iron compression block makes on the snow surface a hole with vertical wall as shown in Fig. 5 **b**. On the spray figure there appears

below the bottom of the hole a deeply tinted region sharply distinguished from the surrounding snow mass. Judging from the spray figure the snow outside the tinted region seems to have undergone no change in structure. The tinted region (region of compressed snow) must be made by the accumulation of the fragmental snow which would have been squeezed out by the destructive contraction if the snow had been compressed in the form of a pillar instead of a large block.

§ 17. The record of the resisting force of snow.

The force with which the snow pillar or snow block offers resistance to compression was registered by a recording galvanometer or by an electromagnetic oscillograph. Most of the registering was made by means of the recording galvanometer for it was convenient in manipulation. But it had a weak point in that it could not exactly follow the rapid change of the resisting force because of its large inertia, that is, of its large time constant. Therefore an electromagnetic oscillograph of very small time constant which could display even the minutest change in the resisting force was sometimes used in order to bring to light the possible matters missed by the recording galvanometer.

No essential difference was found in the resisting force whether the snow was used in the form of a pillar or of a large block.

Examples of registered curve of the resisting force are shown in Fig. 6 and Fig. 7. The curves in Fig. 6 are those obtained by the recording galvanometer while those in Fig. 7 are the ones registered by the oscillograph. The uppermost curve **a** of Fig. 6 shows the case of plastic contraction when the snow was compressed at a very low speed. The compressing iron block was applied to the snow at point A. The resisting force began to rise rather rapidly but soon it came to increase slowly at a constant rate. If the compressing iron block had continued to descend the resisting force would have increased without limit or would have suddenly been diminished due to the appearance of fracture in the snow. Indeed it was sometimes observed that the snow pillar was cut vertically into halves when compressed too much. But in the above case of Fig. 6, **a**, the compressing iron block was stopped at point B when the plastic contraction of the snow pillar had amounted to 16%. As soon as the compression was stopped the resisting force began to decline indicating that the phenomenon of stress relaxation started due to the flowing property of the snow.

Curve **a** of Fig. 6 appears somewhat rugged. But this ruggedness must have originated from some stiffness inherent to the movement of the needle of the galvanometer; it should not be considered as a property proper to the actual resisting force. When the resisting force was registered by the electromagnetic oscillograph whose movement is smooth by nature the curve appeared entirely smooth with no sign of ruggedness, as shown in the uppermost curve **a** of Fig. 7.

Curve **a** of Fig. 6 shows the same form as that obtained by LANDAUER who

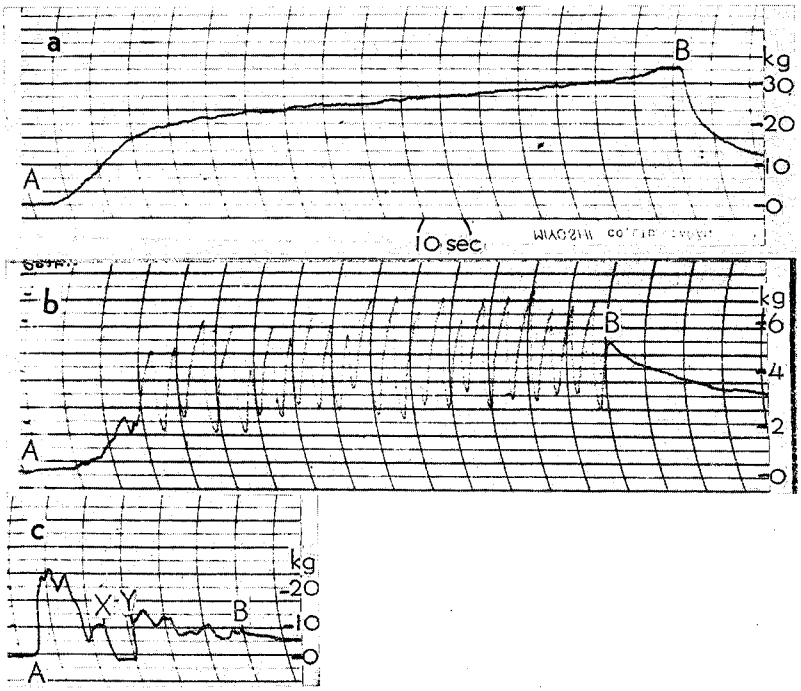

Fig. 6 Curves of resisting force of snow registered by the recording galvanometer. Compression was started at point A and stopped at point B.

a. Plastic contraction of a snow pillar. Compressing speed: 5.7 mm/min. Density of snow: 0.38 gr/cm.^{3}. Temperature: -4°C. Diameter of the pillar: 4.2 cm. The height of the pillar was reduced from its initial value 9.5 cm to 8 cm.

b. Destructive contraction of a snow pillar. Compressing speed: 3.3 mm/min. Density of snow: 0.28 gr/cm^3. Temperature: -10°C. Diameter of the pillar: 6.6 cm.

c. Destructive contraction of a snow pillar at a high speed. Compressing speed: 30 mm/min. Density of snow: 0.38 gr/cm^3. Temperature: -3°C.

made detailed studies on the stress-strain relations in snow under uniaxial compression (*4*).

When the snow was compressed at a high speed so as to undergo destructive contraction the recording galvanometer gave such a curve of resisting force as shown in the middle figure **b** of Fig. 6. The curve oscillates largely up and down but is completely continuous with no break anywhere. But when the oscillograph was used to register the resisting force in place of the recording galvanometer, the curve showed the appearance as in the middle figure **b** of Fig. 7. The curve of resisting force turned out to be a sequence of many segmental lines rising obliquely with sharp discontinuity between them. The actual mode of change in the resisting

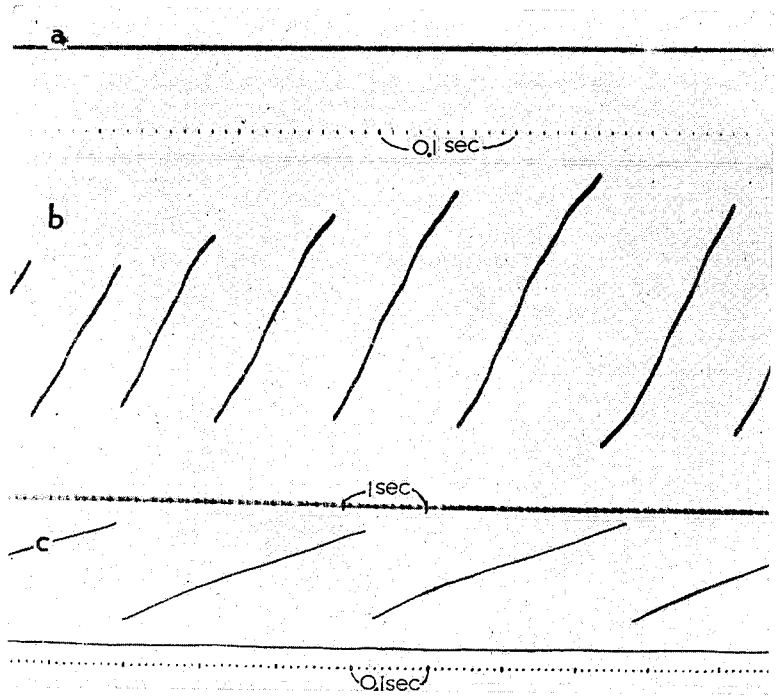

Fig. 7 A portion of the curve of resisting force registered by the oscillograph.

a. Plastic contraction. Curve is quite smooth with no sign of fluctuations.

b. Destructive contraction. This curve was obtained under nearly the same conditions as those of **Fig. 6, b.** The resisting force rises up to a certain value and then suddenly drops showing that there occurred a break-down of snow. Curve **b** of **Fig. 6** did not show such a sudden drop of resisting force decisively.

c. Destructive contraction at a high speed. Portion XY of curve **c** of **Fig. 6** revealed such an appearance when the registering instrument was changed from the galvanometer to the oscillograph.

force must have been such that it rose to stress the snow up to a certain limit R^* where the snow could no more endure the stress and was broken down within a certain portion of the sample. With the break-down the resisting force was momentarily dropped from R^* to a small value R_*, but the remaining unbroken mass of snow began at once to resist the compression again. The saw-toothed feature of the curve must have been given by repetition of such a process. The break-downs of a certain portion of snow evidenced here by the breaks of curve of resisting force must coincide with those described in the previous section, that is, those occurring at the end plane of the snow pillar or at the bottom of the compressed

region of snow in the case of the large block of snow. The recording galvanometer could not follow instantaneously the rapid drops of the resisting force at the break-downs, exhibiting them not by breaks of curve but by steeply declining continuous lines as in Fig. 6, **b**. FURUKAWA and SHIRAI (*2*), SAITO (*3*) had also observed intermittent sharp declines of the resisting force in their experiments of compressing snow, although they had not used a device to register continuously the resisting force.

It should be noticed that the average value of the resisting force is much smaller in the case of curve **b** than in the case of curve **a** (note the difference between the scales of resisting force in both the cases of curves **a** and **b** of Fig. 6); one will experience smaller resistance from snow when he applies force more rapidly.

When the snow was compressed faster than in case **b** of Fig. 6, the recording galvanometer gave the curve of resisting force of such a form as shown in the lowest figure **c** of Fig. 6. It runs irregularly up and down but it looks quite continuous. It may be supposed that the resisting force by being subjected to the large increase in compressing speed recovered the continuous character which it had once lost on the way of increase of the speed. But this is not the case. When the small portion between X and Y of the curve **c** of Fig. 6 was registered by the oscillograph in place of the recording galvanometer it disclosed its saw-toothed feature as shown in the lowest figure **c** of Fig. 7. It is evident that there is no essential difference between the modes of contraction of cases **b** and **c** of Fig. 6. The only difference existing between the two is that the saw-teeth are lower and narrower (counted by time; notice the difference of scale of time in figures **b** and **c** of Fig. 7) in case **c** than in case **b**. The recording galvanometer failed entirely in registering such fine saw-teeth in case **c** due to its large inertia and it could draw only the general trend of the change in the resisting force.

The authors studied previously the resisting force of snow against a heavy body dropped into it (Part III of this series). In that case the falling body compressed the snow at such large speeds as thousands of times those of the present experiments. When compact snow was used for experiment the resisting force of the falling body changed violently during the short time interval of the fall (abuot 0.1~0.2 sec) with a train of high peaks at the beginning. Judging from the likeness seen in both the cases in the form of resisting force curve (cf. Fig. 6 of this paper and Fig. 19 of Part III of this series of papers) and in the spray figure on the cut surface of the snow block subjected to the compression (cf. Fig. 5, **b** of this paper and Fig. 3 of Part III of this series of papers), it may be supposed that there is little or no essential difference between the mechanism of contraction of the two cases. However high the compressing speed may be raised, only a slight modification if any will occur in the mechanism once the speed has exceeded a certain critical value.

§ 18. Transition of the type of contraction with change in the speed of compression.

As described in the preceding two sections, the snow undergoes the plastic contraction with continuous resisting force in the case of low compressing speed, while the destructive contraction occurs on it when compressed at a speed exceeding a certain limit, the resisting force showing saw-toothed features. Now let the mode of transition of the resisting force from the saw-toothed type to the continuous one with decrease in compression speed be considered.

With the decreasing compressing speed each of the saw-teeth becomes higher and broader; the maximum value R^* of the resisting force becomes larger while the time interval t^* during which the resisting force grows from its minimum value R_* to its maximum R^* becomes longer. At the same time the obliquely rising segmental line of the saw-tooth begins to show the tendency to bend downwards as if it were trying to take the form of curve **a** of Fig. 6. When the compressing speed is reduced to a certain critical value the rising curve of the saw-tooth becomes so elongated laterally that no sudden drop of the curve is observed within the time of experiment (a few minutes). The whole curve of resisting force has been covered by a single saw-tooth which is now so deformed that it may not be appropriate to call it "saw-tooth" in the ordinary sense. Here the destructive contraction changes into the plastic one. The visual observation of the snow pillar also shows that the destructive contraction has stopped here; snow has ceased to be squeezed out from the end of the pillar. The above explained mode of transition in the type of contraction will be more clearly understood by its schematic representation shown in Fig. 8.

The transition point from one type of contraction to the other determined in the above-stated way is, however, only a conventional one in the sense that it depends on the time of the experiment. If the experiment is continued longer than for a few minutes the drop of resisting force may still appear at that compressing speed at which the transition occurred in the above case. In this way the compressing speed of transition may be reduced to zero if the time of experiment is prolonged without limit. If so, there will be found no compressing speed of the moment of transition definitely determinable. But the authors think for the following reasons that there does exist a transition speed which is independent of the time of experiment and has a definite physical meaning.

The snow deposited at the beginning of winter of course forms the lowest layer of the snow cover and continues to be compressed very slowly by the weight of the snow lying above it for more than half a year. But it is never observed to undergo the destructive contraction as long as it lies on the flat ground and is subjected to no other force than the weight of the above-lying snow. As far as the present authors are aware, even the snow layer which lies some distance below the surface of a firn field of a vast snow cap seems to show no sign of destructive

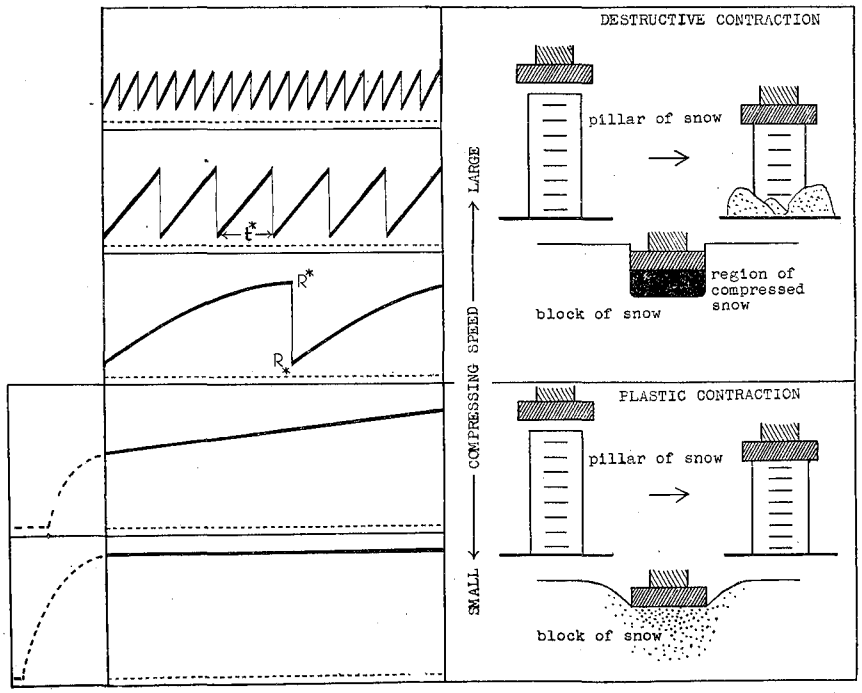

Fig. 8 Schematic representation of the mode of transition of the type of contraction. Compressing speed diminishes from above to below. Figures on the left represent the curves of resisting force while those on the right show the changes in state of snow pillar and block caused by the contraction.

contraction although it may have spent many years under the action of pressure due to the weight of the surface snow layers. Then it may safely be considered that the snow continues the plastic contraction without fracture however long it may be compressed unless the rate of contraction exceeds a certain limit. It was noted in the previous section that instances did occur when the snow pillar was cut vertically into halves when compressed largely, even though it had been contracting plastically up to that time of being cut. In the case of the pillar the stress produced in it by compression deviated slightly from the uniform uniaxial one. The authors suppose that, as the pillar contracted more and more, such a deviation became exaggerated and caused finally the above noted cutting of the pillar. In the ideal case of an infinitely vast uniform snow field where the stress is quite uniform and uniaxial such a cut will never occur in the snow.

In Part II of this series of papers it was shown that the mechanical property of snow could be represented by a rheological model composed of a MAXWELL model and a VOIGT model in series connection so far as the snow was acted upon

by compressive force not so large as to break it down. It was noted there also that such a model could be replaced by a single MAXWELL model (a MAXWELL model is shown in the left portion of Fig. 9) if no high precision was required. Now let the above described mode of transition of the type of contraction be considered on the basis of a single MAXWELL model.

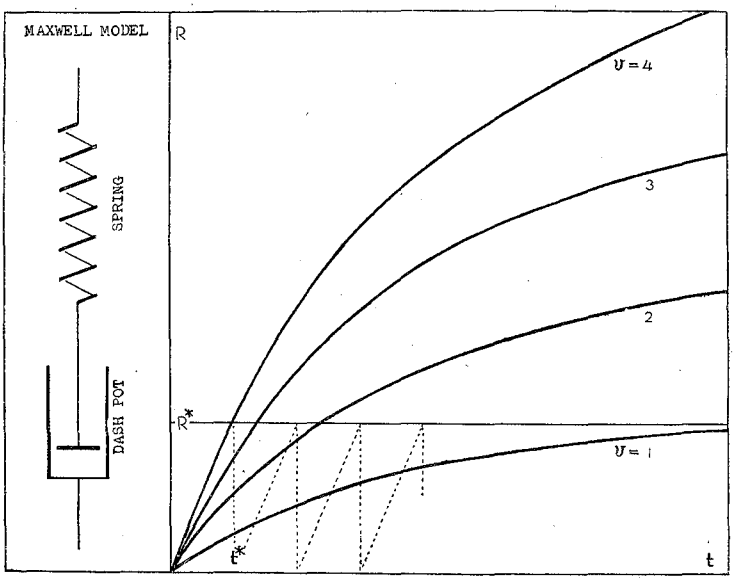

Fig. 9 In the left portion is shown a MAXWELL model. The thick curves in the right portion show the resisting force R of the MAXWELL model when it is compressed at constant speeds of different magnitudes. R^* is the critical stress at which the spring of the MAXWELL model is assumed to give way. The saw-toothed dotted curve represents the resisting force of snow subjected to the destructive contraction. The curve marked $v=1$ is the transition curve which has the largest value of v among those belonging to the plastic contraction. In the case of this figure v^* is taken to be equal to 1.

When a MAXWELL model is compressed at a constant speed v, it offers resistance to the compression with a force R which grows according to the following formula

$$R = AE\tau v\left\{1-\exp(-t/\tau)\right\}, \qquad (1)$$

where E and τ are the elastic constant and the relaxation time of the model respectively while A denotes a constant having the dimension of area. The relation between R and the time t is graphed in Fig. 9 for different values of the compressing speed v. The larger v is, the larger is R and the final value of R which is attained after a long time is equal to $AE\tau v$. It will be natural to assume that

the spring of the model will be destroyed when R reaches a critical value R^* because R is nothing but a manifestation of the stress in the spring. Then, if v is large as in the case of the curve marked $v=4$ of Fig. 9, R will soon (after time t^*) reach R^* and the spring will be broken with the result that R will be suddenly reduced to zero. If an actual MAXWELL model is being dealt with no further process can be considered. But here the MAXWELL model is used only for representing the mechanical property of snow. Then the above described break-down of the spring corresponds to that of the thin snow layer at the end of the snow pillar or at the bottom of the region of compressed snow in the case of snow block. With the break-down of such a layer the remaining snow will be released from stress and its resisting force R will temporally drop. But the remaining snow is at once caught by the compressive force again and begins to resist it in the same manner as the MAXWELL model does. Then R will after the time t^* reach R^* for the second time and the next thin layer of snow will be broken down. In this way the resisting force R of snow will change in the manner represented by the saw-toothed dotted curve of Fig. 9. As shown in the previous section the snow actually exhibits the resistance of such a saw-toothed feature when it is subjected to destructive contraction in the case of high compression speed. As will be seen from the curves of Fig. 9 the time interval t^* needed for R to reach R^* is prolonged with the decreasing speed v. And there will have to arise at one value of v such a circumstance that the curve of R never reaches R^* however long the compression is continued. Such a critical value of v is given by

$$v^* = R^*/AE\tau\,. \qquad (2)$$

It is obvious that all the contraction of snow proceeding at a speed smaller than v^* brings about no break-down and belongs to the category of "plastic contraction". In this way, if the mechanical property of snow is represented by a MAXWELL model, a definite transition value v^* of compressing speed can be found which does not depend on the duration of experiment and does have a definite physical meaning.

In other words, v^* is such a speed of compression that the time interval t^* becomes infinitely long. Therefore it will be necessary to continue the compression of snow infinitely long in order to determine the exact value of v^* by the experimental method. But the time of experiment can not practically be prolonged beyond a few minutes. Then the most which can be done experimentally is to determine whether t^* is longer than the time of experiment or not. But when there is found such a compressing speed v' at which the resisting force of snow ceases to drop within the time of experiment, that speed will not be much different from the true transition speed v^*, as will be seen below.

It was shown in Part II of this series of papers that the relaxation time τ of compact snow is generally a few minutes. Therefore τ is nearly equal to the time of experiment and the ratio t^*/τ will take a value near to one when the drop of

resisting force R comes for the first time not to be observed during the experiment by the lowering of the compressing speed to v'. Equations (1) and (2) yield the relation between t^*/τ and v/v^*

$$-t^*/\tau = ln\left\{1-1/(v/v^*)\right\} \qquad (3)$$

which is graphed in Fig. 10. The curve in the figure rises steeply in the range where t^*/τ, as well as v/v^*, takes values near to unity. Such a situation indicates that v'/v^* is not far different from unity, that is, v' nearly equal to v^*, so long as the value of t^*/τ is kept in the vicinity of unity. The last condition is fulfilled in the experiment as noted above. Therefore that compressing speed v' at which no drop comes for the first time to appear on the resisting force as a result of the lowering of v can be taken as an approximate value of v^*.

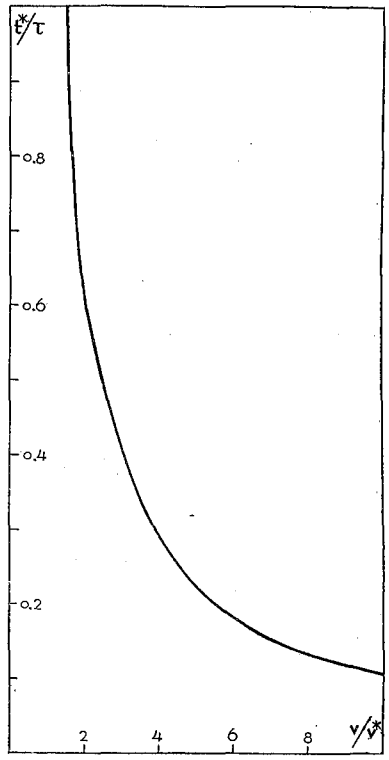

Fig. 10 Relation between t^*/τ and v/v^*.

The representation of the mechanical property of snow by the single MAXWELL model gives, as described above, a good explanation to the main features of the contraction of snow at constant speeds. It explains the elongation of t^* with the decreasing compression speed v and also the mode of transition from the destructive contraction to the plastic one. But it fails to account for the increase of the average value of resisting force $\bar{R}$ with the decrease of compressing speed v. The authors have found that the actual snow is more precisely represented when a series of MAXWELL' models is used in place of a single one. They are hoping also to explain in the future the increase of $\bar{R}$ with decreasing v by making use of such a series of models.

§ 19. Details about the contraction of snow at constant speeds.

(1) Work-hardening of snow by compression. It was shown in Part II of this series of papers that the snow becomes elastically hard by increasing its YOUNG's modulus when it is subjected for some time to the action of compressing force, even if the force is kept far below the yielding point of snow. The gradual increase of resisting force of snow in the later stage of plastic contraction described in the previous sections indicates that the snow becomes hard as a result of plastic

contraction. Although such a phenomenon of work-hardening of snow has not been considered until now it must to a greater or less extent have been taking place in all the snow used in the present experiments. It disclosed itself most conspicuously when the snow was compressed at the transition speed v^*. Fig. 11 shows the resisting force which is exhibited by a block of snow compressed at a speed near to v^*. It began to contract in the form of "destructive contraction," but the peak value R^* of the resisting force tended to increase as the contraction proceeded, which fact shows that the snow gradually became hard. Finally the resisting force discontinued dropping and thereafter the type of contraction changed into the "plastic" one as shown in Fig. 11. Such a transition of contraction from the destructive type to the plastic one was often observed when the snow was compressed at a speed near to the transition value.

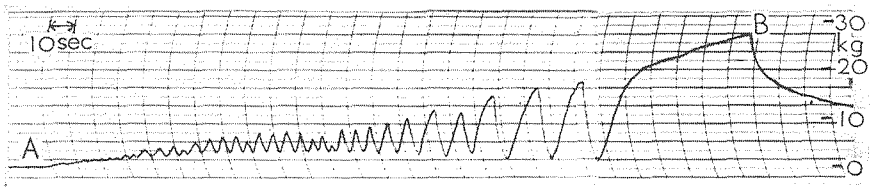

Fig. 11 Snow often changes the type of contraction from the destructive to the plastic when compressed at a speed near to the transition speed v^*. In case of this figure a metal plate (diameter: 5.9 cm) was forced into a block of snow (density: 0.28 gr/cm^3, temperature: -4.8°C) at the speed 3.3 mm/min. A hole 1.3 cm deep was made with the region of compressed snow 1.3 cm thick below its bottom.

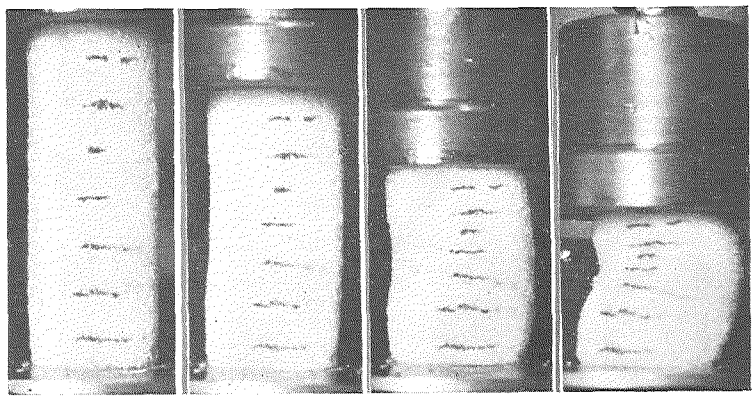

Fig. 12 Snow pillar deformed by a large plastic contraction. Density of snow: 0.30 gr/cm^3. Temperature: -16°C. Compressing speed: 1.9 mm/min.

Work-hardening is not the only change which is observed on the pillar of snow under compression; the pillar undergoes change in the lateral dimension besides that in the longitudinal length which is the proper consequence of the experiment.

Fig. 12 illustrates the change in the form of snow pillar which was subjected to a large plastic contraction. The pillar thickened except near the top and bottom where it was prevented from thickening by the end metal plates; it had lost its uniformity of thickness. The pillar was also bent, which must have brought about a complicated distribution of stress throughout the snow. When the pillar was deformed to such a large extent its contraction would be very different from the uniaxial uniform contraction which is the subject of the present study. Therefore the experiments of registering the resisting force were generally discontinued when the pillar contracted to such a state as shown by the second photograph from the left in Fig. 12.

(2) *Enlargement of the resisting force with the decrease of the compressing speed.* The average resisting force $\bar{R}$ of snow against compression is raised as the compressing speed v is lowered. In case of "destructive contraction" the maximum value R^* of the resisting force rises with lowering speed. Fig. 13 shows most clearly such a situation. There the compressing speed was suddenly enlarged at point C and R^* was reduced to less than the half of the prior value. In case of "plastic contraction" it is impossible to give in the strict sense a definite magnitude to the

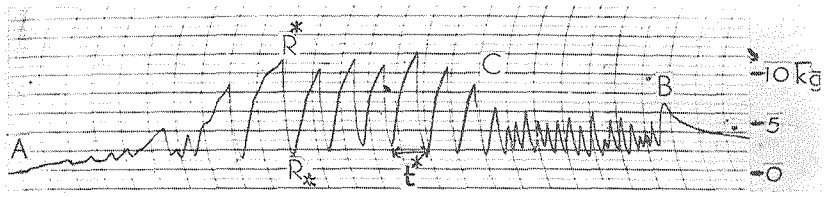

Fig. 13 The resisting force of snow undergoing the destructive contraction is reduced when the compressing speed is increased. Here the compressing speed was enlarged suddenly at point C from 1.1 mm/min to 2.75 mm/min. Pillar of snow of the diameter 5 cm. Density of snow: 0.28 gr/cm^3. Temperature: -22.2°C.

resisting force for it continues to increase as long as the compression is maintained. Then the present authors use for the sake of convenience as a measure of its magnitude the value which the resisting force attains at the end of the experiment, that is, the maximum value observed in the experiments. Then R is found to be generally larger for "plastic contraction" than for "destructive" one. The above described circumstances are clearly indicated in Figs. 14 and 15 which show the dependency of the resisting force p per unit area on the compression speed or on the time rate of change in the strain of snow pillar.

(3) *A single saw-tooth of the curve of resisting force becomes narrow with increase in the speed of compression.* The time interval t^* between the adjacent two drops appearing in the saw-toothed curve of resisting force of snow subjected to "destructive contraction" becomes short as the compressing speed v is increased. This is shown in Fig. 16. As mentioned before, in the case of "destructive

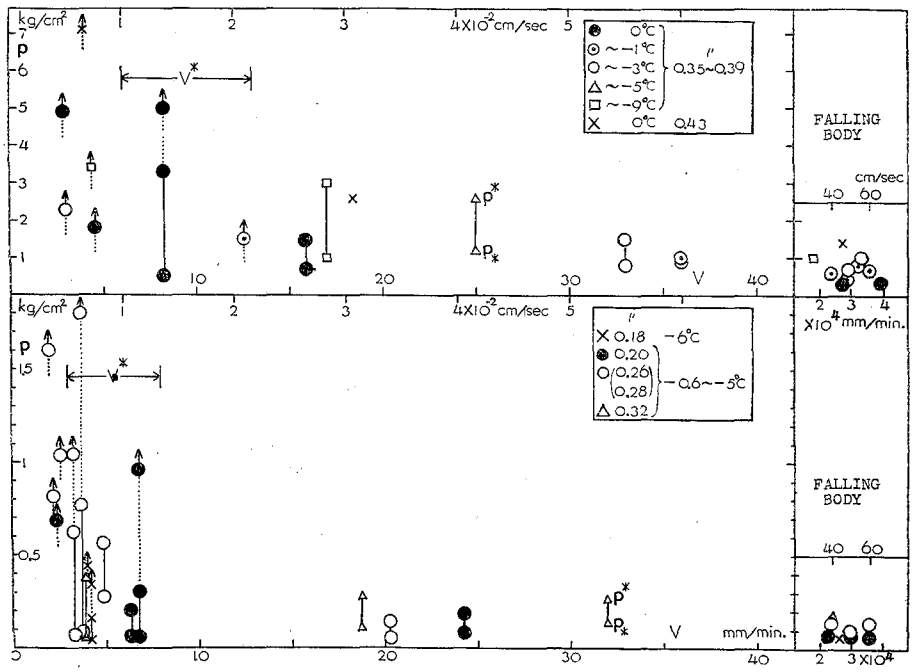

Fig. 14 The resisting force p per unit area ($=R/A$. A: compressing area) is plotted against the compressing speed v for the case of snow block. A mark with an arrow and a dotted segment lying in the left portion of the figure shows the maximum value of p which the snow shows, being subjected to the plastic contraction, at the end of the compressing experiment. The arrow indicates that p will be increased more and more if the experiment is continued further. Two marks joined by a thick segment show the range in which p fluctuates at the destructive contraction, the top mark being p^* ($=R^*/A$) and the bottom one being p_* ($=R_*/A$). The transition speed v^* is not shown by a point but by a range since it is not of the nature to be determined definitely. A group of three marks joined by a thick line and a dotted one with an arrow at its top belongs to the case in which the type of contraction changes from the destructive to the plastic during the time of experiment. An example of such a case is shown in Fig. 11. The lower two marks show p^* and p_* of the last saw-tooth at the end of the period of the destructive contraction while the top mark indicates the value of p at the end of the experiment when the snow is undergoing the plastic contraction. The marks within the separate enclosure at the right extremity of the figure give the average resisting force which the snow exhibits against a body falling into it (cf. Part III of this series of papers). In case of the falling body the compressing speed v is very large, thousands times as large as that used in the present compressing experiment, but the resisting force remains still of the same order of magnitude as that of the destructive contraction at a low speed.

The density and temperature of snow are indicated by giving different shapes to the marks. The correspondence between the density, the temperature and the shape of mark is shown in the rectangular enclosures. The upper half of the figure contains hard compact snows of the density larger than 0.35 gr/cm³ while the lower half contains soft compact snows of smaller densities. The transition compressing speed v^* ranges 6~13 mm/min for hard snow and 3~8 mm/min for soft one.

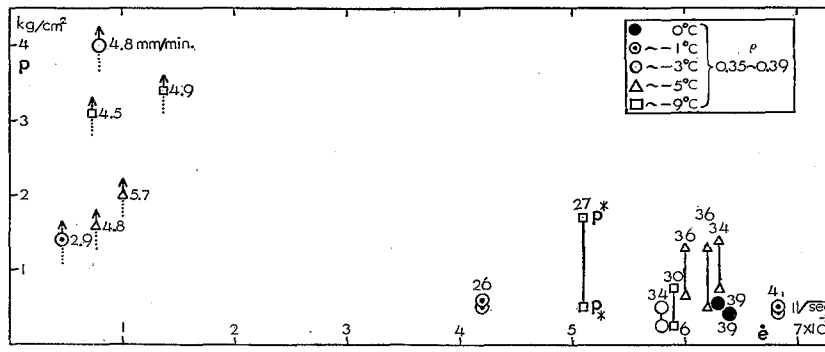

Fig. 15 The resisting force per unit area p is plotted against the time rate of change $\dot{e}$ in the strain of contraction undergone by snow pillars. $\dot{e}$ is the same thing as v divided by the height of the snow pillar. The numerical figures attached to each of the marks show the compressing speed v in the unit of mm/min.

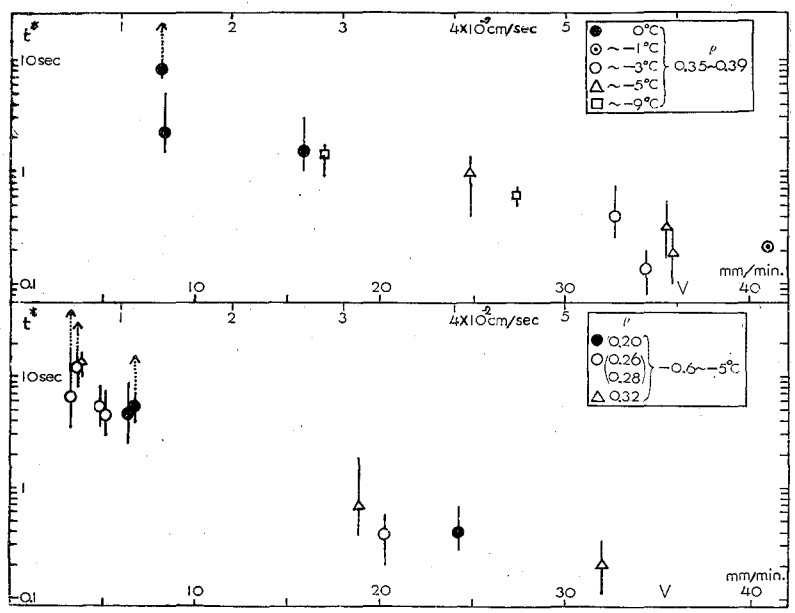

Fig. 16 t^*, the time interval between two adjacent drops in the saw-toothed curve of resisting force of the destructive contraction, versus v, the compressing speed. Since t^* is not the same for each of the saw-teeth the mark indicating its mean value is attached with a segment which shows the range of distribution of values of t^*.

contraction," the destruction occurs step by step in a thin snow layer located at the end of the snow pillar or below the bottom of the region of compressed snow in the case of the snow block. Every time a thin layer is broken down there

appears a drop in the resisting force. Therefore the thickness of the thin snow layer which is destroyed at that moment is given by $x^*=vt^*$. There is also decrease in x^* with the increasing compression speed v as shown in Fig. 17, though not so conspicuously as in t^*. (Note that t^* is counted in Fig. 16 by the logarithmic scale while x^* in Fig. 17 is by the linear scale). It should be noticed that x^* is of the order of one millimeter or of its fraction; x^* is at largest several multiples of the linear dimension of the ice grains composing the snow sample.

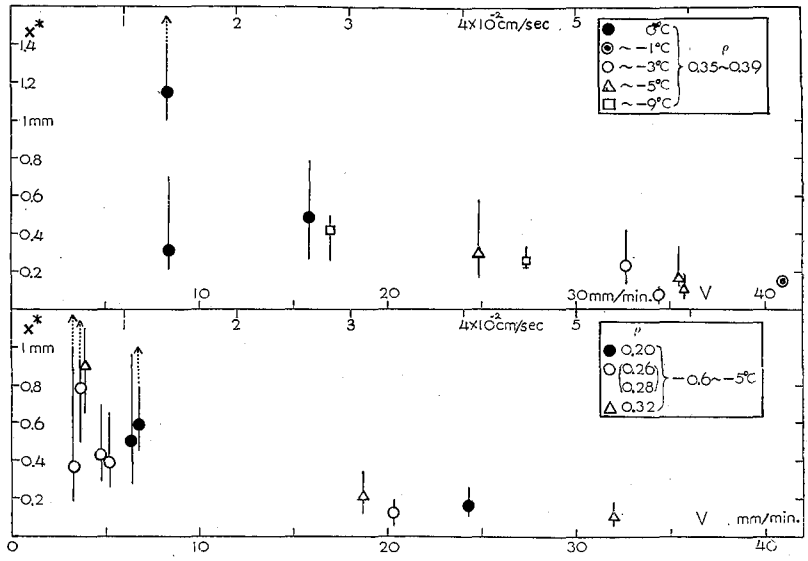

Fig. 17 $x^*=vt^*$ versus v. x^* is nothing but the thickness of the thin snow layer which is broken down at a time by the destructive contraction.

(4) *Relation between the YOUNG's modulus E of snow and the compressing speed v.* When a snow pillar of height l is undergoing destructive contraction, no large flow will occur in the snow during the time interval t^* since t^* is very short. The snow can be considered as an elastic body of which the stress grows from p_* to p^* during that time interval. (The stress p is given by the resisting force R of the snow pillar divided by its sectional area.) Then (p^*-p_*) divided by (x^*/l), the increase in the strain of snow pillar during t^*, yields the YOUNG's modulus E of the snow. In the case of the snow block E is determined in the following way. When the surface of a semi-infinite elastic body is pressed by a circular rigid plate of diameter D with force R, the rigid plate penetrates into the elastic body by an amount given by

$$x=\frac{(1-\sigma^2)R}{DE}, \qquad (4)$$

where σ is the POISSON's ratio. The situations are not exactly the same in the above

case of the elastic body and in the case of compressing the snow block, but the difference between the two seems to be rather small. Therefore the present authors take advantage of formula (4) for determining the YOUNG's modulus E of snow by means of replacing x and R in formula (4) by x^* and R^*-R_* respectivery. $(1-\sigma^2)$ can be put equal to unity taken as a whole since it has been shown by BUCHER (6) that σ of snow is as small as 0.2. Then the formula useful for obtaining the YOUNG's modulus of the snow block is given by

$$E = \frac{R^*-R_*}{Dx^*}, \tag{5}$$

where D is the diameter of the iron block used for compressing the snow block.

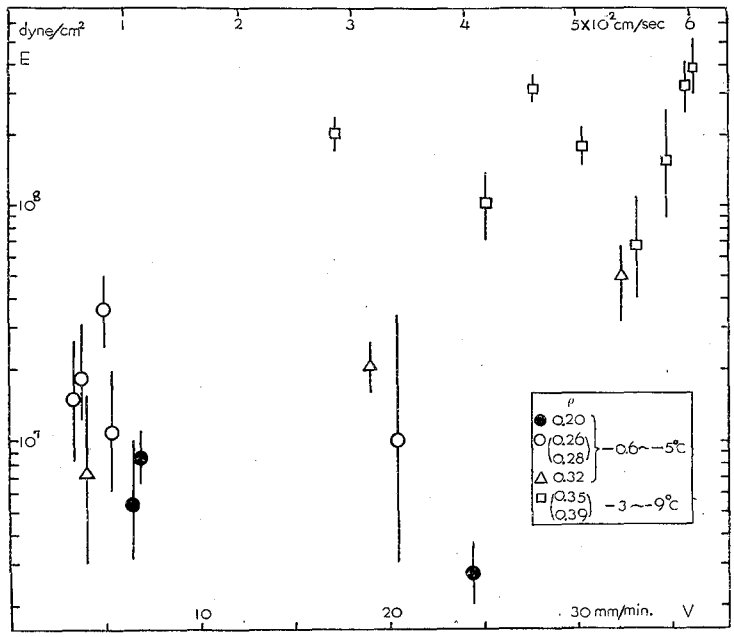

Fig. 18 YOUNG's modulus E of snow obtained from the saw-toothed curve of resisting force of destructive contraction versus compressing speed v.

The YOUNG's modulus E of snow determined in the above-described way is shown in Fig. 18 in dependence on the compressing speed v. E shows a tendency to increase with the increasing v. The values of E are found to be of the order of 10^7 or 10^8 dyne/cm^2 in accord with those determined before in the statical experiments performed by the present authors (§2 of Part II of this series of papers).

(5) *Frequency distribution of R^*, R_*, t^*, x^*, E, quantities which characterise each of the saw-teeth composing the curve of resisting force of the destructive contraction.* The saw-teeth composing the curve of resisting force of snow under-

going destructive contraction are shaped somewhat differently from one another as seen in the figures shown in Fig. 6, **b** or in Fig. 7, **b**. Therefore the values of their characteristic quantities such as R^*, R_*, t^*, etc. spread within a range with different frequency of occurrence for different values of the quantities. The upper figure of Fig. 19 shows a portion of a saw-toothed curve and below it are shown the histograms of the characteristics of the saw-tooth obtained from the former. The ranges of the value of characteistics are rather wide, which may partly be caused by the fact that the curve of resisting force has an irregular wavy trend as seen in the upper figure of Fig. 19. The snow is composed of layers having different structures even when it looks perfectly uniform in outer appearance and such a non-uniformity in the structure of snow must have caused the wavy trend of the curve.

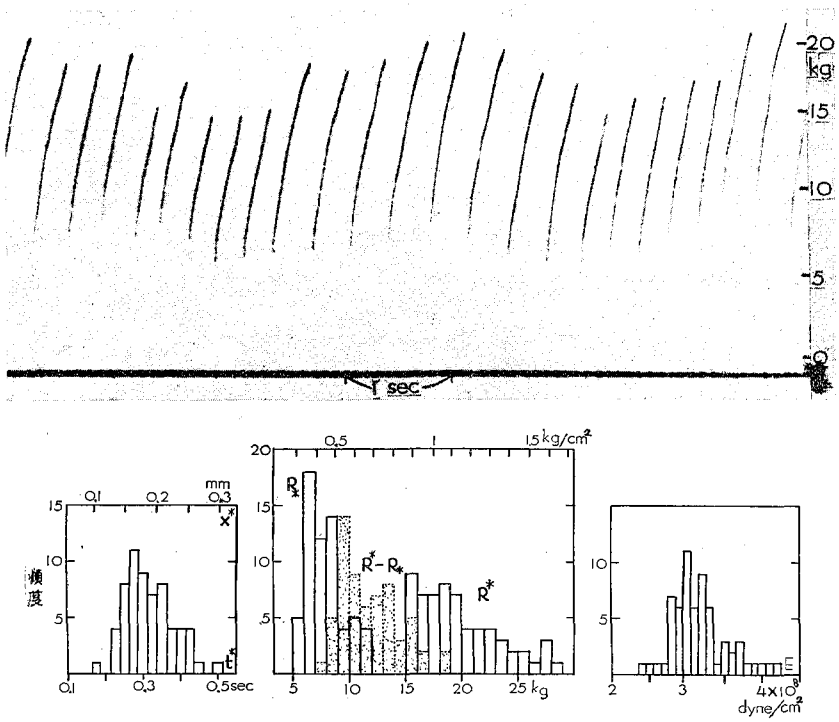

Fig. 19 Top: saw-toothed curve of destructive contraction registered by the oscillograph. Snow pillar of the density 0.36 gr/cm³. Temperature: −4.5°C. Compressing speed: 35 mm/min.
Bottom: frequency distribution of the characteristic quantities of saw-teeth of the top curve. R^*-R_* is the depth of drop from the top edge of the saw-tooth.

When a snow block is laid sideways in such a way that the snow layers composing it stand upright and it is compressed from above, the saw-toothed curve of

resisting force comes to take such a uniform appearance as shown in the top of Fig. 20. The histograms in the same figure obtained from the top curve show that the characteristic values spread in ranges narrower than those of Fig. 19. In the case of snow block laid side-ways the structure of snow is uniform in the direction of compression, which fact must have caused the irregular wavy trend to disappear from the resisting force of Fig. 20. It should be noticed that a similar thing occurred to the resisting force of snow against a body falling into it; the block laid sideways resisted the falling body with a nearly constant force (§9 of Part III of this series of papers).

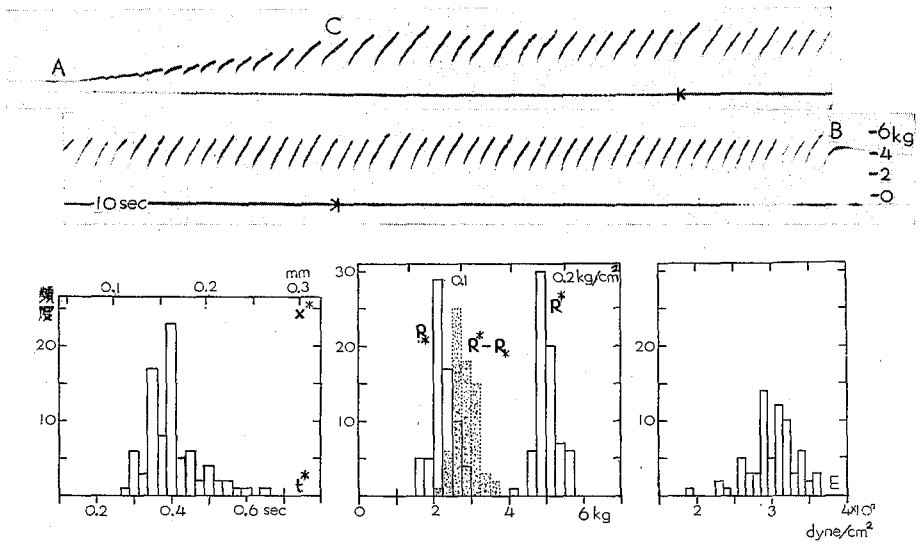

Fig. 20 Top: saw-toothed curve of destructive contraction registered by the oscillograph. Snow block of the density 0.20 gr/cm³ so laid that the snow layers composing the block stand upright. Compression proceeded parallel to the snow layers giving a regular saw-toothed curve of resisting force. Temperature: −3.7°C. Compressing speed: 24 mm/min.
Bottom: frequency distribution of the characteristic quantities of saw-teeth of the top curve.

(6) *The coefficient of viscosity η as affected by the "plastic contraction"*. What is called here "coefficient of viscosity η" is the ratio $p/\dot{e}$ in the case of plastic contraction. p is the resisting force of snow per unit area in the stage where the resisting force increases gradually with time after the rather steep rise of the force at the beginning of compression has finished (see Fig. 6, **a**). $\dot{e}$ is the time rate of change in the strain of the snow pillar which is equal in amount to v/l (v: compressing speed, l: height of the pillar). By the same reason as that which yielded formula (5) of article (4) of this section, in the case of the snow block, η is given

by the formula $\eta = p/Dv$, where D is the diameter of the iron block used for compressing the snow.

In Fig. 21, η is plotted against the density ρ of snow. η increases with the increase of ρ. Every two of the marks in the figure joined by a line to form a pair indicates the range within which η changes in one and the same experiment. The value of η increases from the bottom mark of the pair to the top one in the whole course of the gradual increase of the resisting force following the first rise.

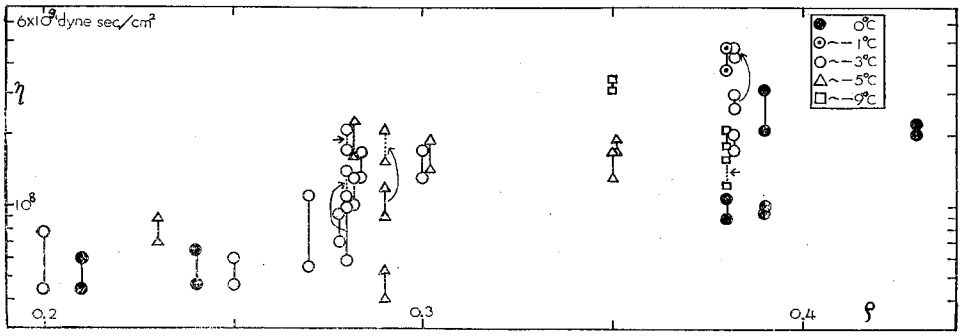

Fig. 21 Coefficient of viscosity η versus density of snow ρ. Plastic contraction. The value of η increases from the bottom to the top of the pair of marks joined by a line during the period of gradual increase of resisting force following the first period of steep rise. When the plastic contraction is interrupted and resumed, the range of value of η is shifted upwards by that interruption as shown by the arrow.

Fig. 21 shows that η is of the order of $10^7 \sim 10^9$ dyne·sec/cm^2, but the authors found before, in their observation on the natural contraction of snow layers composing the snow cover, that compact snow of density larger than 0.2 gr/cm^3 had η greater than 10^{10} dyne·sec/cm^2 (§3 of Part II of this series). Such a discrepancy between the values of η must have arisen from the differences between the compressing pressures p or those between the time rates $\dot{e}$ of change in strain of snow of the two cases. Indeed $\dot{e}$ was found to be $10^{-6} \sim 10^{-7}$/sec in the case of the natural contraction of snow layers while more than a thousand times larger $\dot{e}$ ($\sim 10^{-3}$/sec) is used in the present experiment. From these numerical figures the value of η is expected to vary in dependence on p or $\dot{e}$ provided that the phenomenon of work-hardening exerts little influence; η will be enlarged as p or $\dot{e}$ is decreased. But the dependency of η on p or $\dot{e}$ seems to become very weak, that is, η seems to tend to become constant, when p or $\dot{e}$ is very much reduced. As will be shown in the later sections the depth of snow cover as well as the distribution of density within it can be computed from the data of snow falls in the past under the assumption that η is independent of p or $\dot{e}$. Then the snow may be considered to be plastic when it is compressed rather slowly and viscous when compressed very slowly. Hence the present authors call the continuous slow contraction dealt with

in the present experiments "plastic contraction" while they have called the contraction observed on the snow layers composing the snow cover "viscous contraction". (In § 3 of Part II of this series of papers, "viscous compression" was used instead of "viscous contraction").

If the plastic contraction of snow is once discontinued and then resumed after an interruption, it is found that η has been enlarged during the interruption. Such a phenomenon is indicated in Fig. 21 by two pairs of marks connected by curved arrow. The same phenomenon was observed also in the experiments which the authors performed by compressing snow pillar by a small weight (Fig. 12 (d) in Part II of this series).

(7) *The type of contraction and the temperature.* The saw-teeth of the curve of "destructive contraction" is reduced in amplitude as the temperature of snow rises towards 0°C. The same snow which had given the curve shown in Fig. 19 at −4.5°C exhibited the resisting force of Fig. 22 when its temperature was raised to −1°C. Together with the reduction in the amplitude of saw-teeth the drop of the resisting force occurring at the edge of each saw-tooth become gentle in slope; it will be better to designate the curve of Fig. 22 as "zigzag" rather than "saw-toothed". When the temperature reached 0°C the curve of resisting force came to show only very small fluctuations and the snow which by that time was being squeezed out in fragments from the end of snow pillar fused into a thin plate hanging down like a tongue as shown in Fig. 4. But the fusing of the squeezed out snow into the thin plate is not restricted to the cases of the temperature 0°C. When the compressing speed v exceeds a few tens of mm/min such a fusing occurs even below 0°C and the curve of resisting force shows a zigzag feature like that exhibited by the curve of Fig. 22. Let the contraction occurring under such conditions be called "destructive contraction of the second kind".

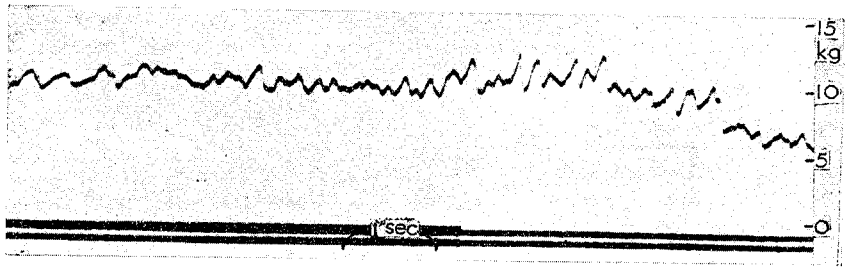

Fig. 22 The curve of resisting force exhibited by the same snow as that of **Fig. 19** changed into such a one as shown here when the temperature was raised up to −1°C. The curve is zigzag rather than saw-toothed.

The contractions undergone by the snow pillars at different compressing speed v and under different temperature T (°C) are represented in the $v-T$ plane of Fig. 23 by the marks placed at points corresponding to the applied v and T. The type

of contraction is distinguished by different shapes assigned to the mark; plastic contraction by a cross, destructive one by a light circle and destructive one of the second kind by a solid circle. The $v-T$ plane can be divided into three domains whithin each of which almost all the marks belong to one and the same type of contraction.

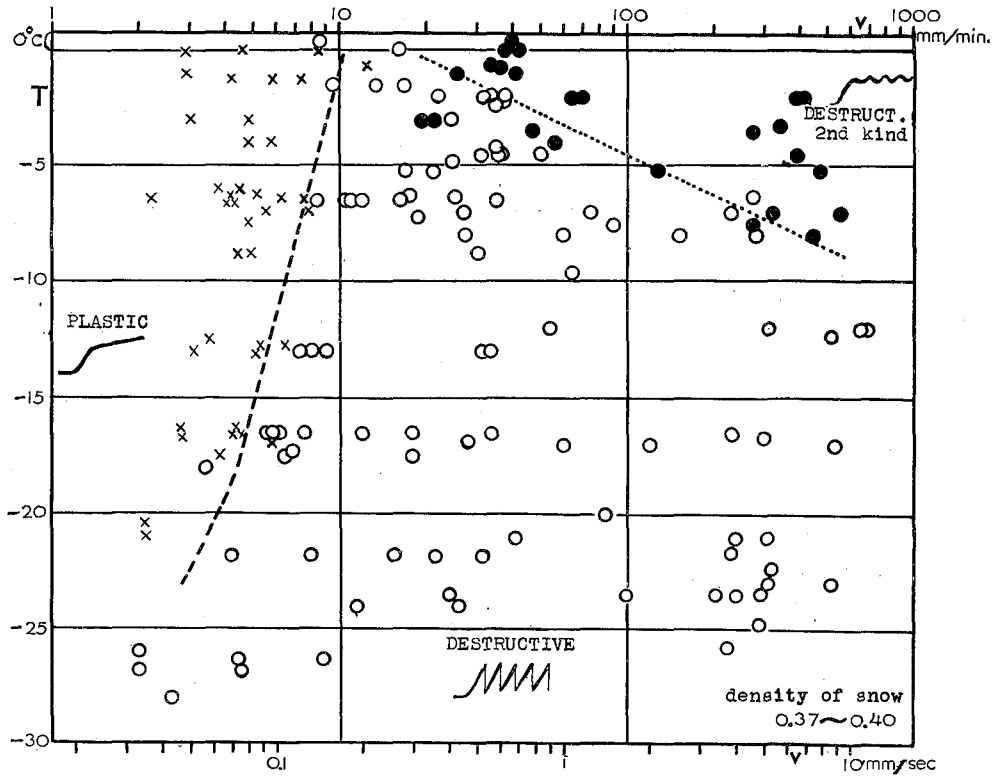

Fig. 23 The type of contraction is dependent on the compressing speed v as well as on the temperature T(°C) of snow. The results of experiments performed with different compressing speeds and temperatures are distinguished in the figure by different marks according to their type of contraction. Cross: plastic contraction, light circle: destructive contraction, solid circle: destructive contraction of the second kind.

Starting from the domain of destructive contraction one will secure the plastic contraction and the destructive one of the second kind respectively by decreasing and increasing the compression speed at one and the same temperature. The latter two types of contraction show curves of resisting force of the like form; they are like each other in that they rise rather steeply for some time after the beginning of contraction and then bend themselves so as to proceed horizontally or slightly upwards thereafter. The only distinct differences are that the resisting force is

much smaller in the case of destructive contraction of the second kind than in that of plastic one and that the curve of resisting force is entirely smooth in the latter case while it shows the zigzag feature in the former. If one uses an instrument of slow action such as a recording galvanometer in registering the resisting force of snow he may not discern such a difference existing in the forms of the curves of the two cases. But that difference is of quite an essential nature: the plastic contraction is produced by the enlargement and the extreme prolongation of one saw-tooth of the destructive contraction while the destructive contraction of the second kind is the result of the reduction in size and the augmentation in number of the saw-teeth of the destructive contraction.

§ 20. A remark on the cause of avalanches.

As well known the snow cover deposited on sloping ground is always creeping downwards along its surface and some authors are of the opinion that the enlargement of the creeping speed is an advance notice of the occurrence of an avalanche. The results of experiments described in the preceding sections to the effect that the resistance of snow against the compression diminishes with the increase of compressing speed may promisingly be used to explain the acceleration of the creep of snow cover and the occurrence of an avalanche. As a general rule an advancing phenomenon develops to an outbreak if the increase of its advancing speed is accompanied by the diminution of resistance.

The snow cover lying on sloping ground is generally in stressed state and subjected to "plastic deformation". In some domains of the snow cover the snow will be undergoing "plastic contraction", the snow mass lying above pressing down upon the one lying below. As the contraction proceeds there will appear within one of the domains such a region in which the compressive stress comes to reach the yield stress to destory the snow. Then the plastic contraction having prevailed in that domain changes into the destructive one. The large resistance to which the snow mass lying above the yielding region has been subjected due to the plastic contraction is now reduced to a small one and the motion of that snow mass will come to be much accelerated. The breakdown of the snow structure which has started from the yielded region will be maintained by the accelerated motion of the above lying snow mass and the broken snow will be squeezed out as in the case of the compressed snow pillar or will be packed as in the case of the compressed snow block. If such a process lasts for some time that snow mass which lay above the yielded region may attain a momentum large enough to set the snow mass lying below also in motion to start an avalanche.

Numerical Computation of the Thickness of Snow Cover from the Amount of Precipitated Snow.

§ 21. Contraction of the snow layers composing snow cover.

The snow cover on the ground is thickened layer by layer by the intermittent precipitation of snow. If each of the snow layers composing snow cover would keep the thickness unaltered as it was at the time of precipitation the whole thickness of the snow cover at any time would be known from the total amount of snow which had precipitated up to that time. But in reality the snow layers shrink as time goes on and, in addition to that, the time rate of contraction of snow layers differs from one layer to another; the precipitated amount of snow and the thickness of snow cover never stand to each other in such a simple relationship as mentioned above. A snow layer tends to contract more rapidly as it lies deeper in the snow cover because it must then support the weight of the larger snow mass resting upon it. But there are other factors which act in the opposite direction to prevent the deep snow layer from rapid shrinkage. The more a snow layer is contracted, the harder it becomes due to the phenomenon of work-hardening described in article (*1*) of the previous section §19. Moreover snow largely alters its structure during a long period such as many weeks or months according to the phenomenon of sublimation-metamorphosis as described in Part I of this series of papers. Such an alteration in the structure also effects the hardening of snow preventing it from being compressed rapidly.

In their effort to find some order if any order exists in the way of shrinking of the snow layers composing snow cover the present authors were able to obtain a simple formula relating the coefficient of compressive viscosity η of snow with its density ρ. Detailed description of this subject has already been given in Part II of this series of papers. The authors develop here a method to compute numerically the thickness of snow cover as well as the density distribution within it from the precipitation data of snow by the use of the above mentioned formula of η and ρ (*7*). They hope by advancing on this line of study to reach a method which will permit determination of the mass of snow laid on the ground by measuring merely the depth of snow cover.

Coefficient of compressive viscosity η of snow is defined by the formula

$$\eta = p/(de/dt), \qquad (6)$$

where p is the pressure acting on a snow layer while de/dt denotes the time rate of change in compressive strain undergone by that snow layer. Practically de is obtained by determining the ratio (amount of shrinkage $-dh$ occurring to a snow layer during one day/average thickness h of that snow layer on that day) which is the same thing as (increment $d\rho$ in the density of snow during one day/average value ρ of snow density on that day). Putting dt=one day, de determined in the above way gives the numerical value of de/dt in the unit of (1/day). The pressure

p is nothing but the weight of snow layers lying above the one in question taken for the horizontal unit area. Such a weight can be determined from the vertical distribution of snow density which is obtained by measuring the snow density of each of the snow layers composing snow cover.

As time goes on both the density ρ and the coefficient of viscosity η of snow layer become greater and the present authors found that these two quantities are connected to each other in a manner expressed by the formula

$$\eta = \eta_0 \exp(k\rho). \qquad (7)$$

In this formula k is a constant having the value 21.0 cm^3/gr common to all snow layers while η_0 changes its value from one snow layer to another within the range 0.6~1.6 gr-wt·day/cm^2 although it comes out to be a constant for one and the same snow layer. That such a formula holds good between η and ρ was ascertained in the case of no less than twenty snow layers composing snow covers deposited in the last three winters (1954–55, 55–56, 56–57) on the flat ground near the authors' Institute. Observed data obtained on some of the snow layers are shown in Fig. 24, η and ρ being counted by logarithmic and linear scales respectively. One will see that the marks of the same shape which belong to one and the same snow layer stand in a line and that the lines belonging to different snow layers run parallel to one another in accord with the above noted formula (7). The three straight lines marked **a**, **b**, **c** in Fig. 24 are those obtained by putting $\eta_0 = 1.6$, 1.0, 0.6 gr-wt·day/cm^2 in formula (7) respectively. The difference between the values of η_0 seems to have arisen mainly from the difference of average temperature of the snow layers, although it cannot be said that the sort of snow crystals fallen from the sky to form the snow layer has no effect upon the value of η_0. Judging from the results of experiments performed in the cold room of the authors' Institute for the purpose of determining the dependency of the viscosity of snow on the temperature, the authors construct the lines **a**, **b**, **c** of Fig. 24 for the temperatures −7°C, −3°C, −1°C respectively.

It should be noticed that such a simple relationship beween η and ρ as described above holds only for a layer of soft snow changing to compact snow so long as its density ρ lies within the range from 0.08 to 0.4 gr/cm^3. Compact snow is, however, never an exceptional sort of snow but is the most general one. During the most part of winter, compact snow is that sort which composes the snow cover. With the approach of spring about the time when the density of compact snow has increased to about 0.4 gr/cm^3, it often begins to change into granular snow due to the partial thawing of the snow cover with the result that the value of $\log\eta$ begins to rise with the increase of ρ more rapidly than it has been doing. This is shown in Fig. 24 by the upward bend occurring to some of the broken lines representing the $\log\eta$—ρ relationship in the upper right portion of the figure. If the compact snow becomes granular not because of the partial thawing but due to the forma-

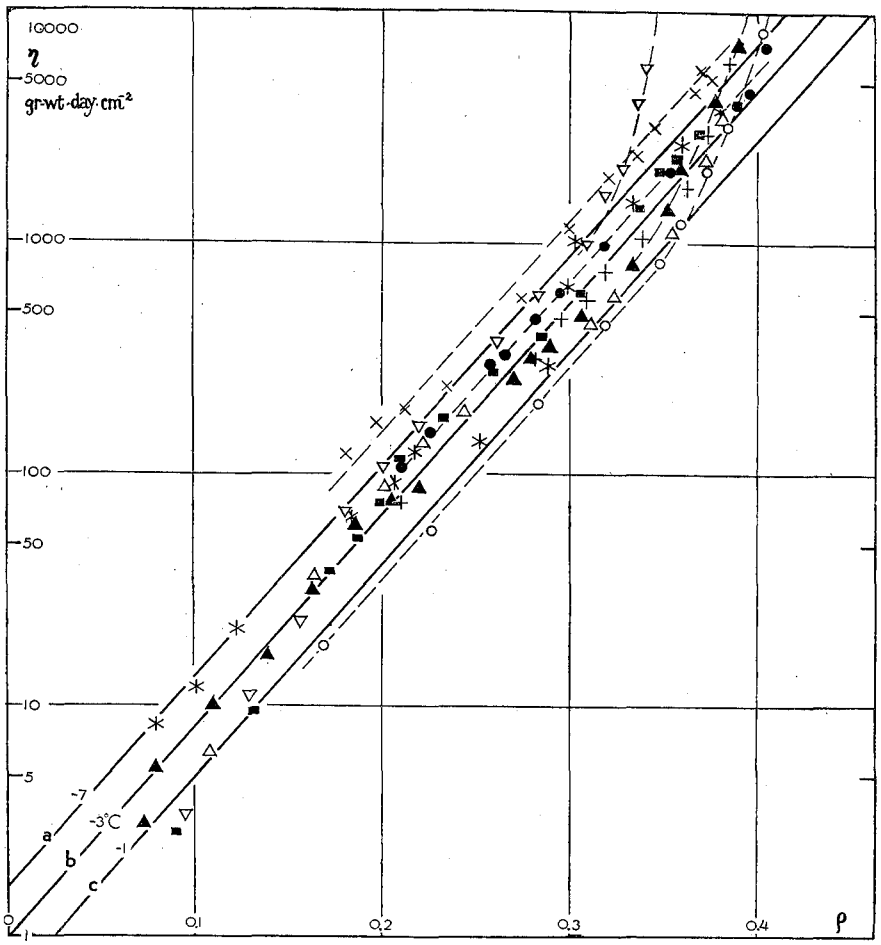

Fig. 24 Coefficient of viscosity η of snow layer and its density ρ. The observed points belonging to the individual snow layers are shown respectively by different marks. $\log \eta$ stands in linear relationship with ρ for all the snow layers, the lines belonging to different snow layers being parallel to one another. The thick lines marked a, b, c show the idealised relationships between $\log \eta$ and ρ corresponding to the temperatures -7, -3, -1°C respectively.

tion of depth hoars such a bend can occur to the $\log \eta - \rho$ curve at the smaller values of density ρ such as 0.15 or 0.2 gr/cm³.

§ 22. Basic procedure for computing the depth and the density distribution of snow cover.

The whole course of computation which will be developed below is based on the assumptions that the snow cover is composed of compact snow and that formula (7) described in the previous section holds good irrespective of however the pressure

acting on the snow layer may be changed in magnitude. Let the time counted from the time of first formation of snow cover on the ground, that is, the time from the commencement of the period of "continuous snow cover" in winter be denoted by t and the snow layer deposited at $t=t'$ be called t'-layer. Then, if the pressure acting on the t'-layer at time $t(>t')$ be denoted by $w(t,t')$, the density $\rho(t,t')$ of t'-layer will change according to the differential equation

$$\frac{1}{\rho}\frac{d\rho(t,t')}{dt}=\frac{w(t,t')}{\eta(\rho(t,t'))}\,, \tag{8}$$

which is nothing but a rewritten form of formula (6) of the previous section used for defining the coefficient of viscosity η of snow. By the aid of formula (7), differential equation (8) is converted to the integral form

$$\eta_0\int_{\rho_0}^{\rho}\exp(k\rho)\,d\rho/\rho=\int_{t'}^{t}w(t,t')\,dt\,, \tag{9}$$

where ρ_0 is the initial value of the density ρ of t'-layer. It will easily be seen that the integral on the left side of this equation is expressible in the term of the logarithmic integral

$$\overline{Ei}(x)=\int_{-\infty}^{x}\exp(u)\,du/u\,; \tag{10}$$

the above integral form (9) then yields

$$\eta_0\left\{\overline{Ei}(k\rho)-\overline{Ei}(k\rho_0)\right\}=Q(t,t')\,, \tag{11}$$

$$Q(t,t')=\int_{t'}^{t}w(t,t')\,dt\,. \tag{12}$$

Let the curve marked $W(t)$ in Fig. 25 represent an "accumulation curve" of snow cover. $W(t)$ is the amount of snow expressed in terms of weight accumulated per unit area of the ground by the precipitations of snow which have occurred up to time t. It is needless to say that the accumulation curve is obtained from the every day data of precipitated snow. Obviously the pressure $w(t,t')$ acting upon t'-layer, being equal to the weight of snow mass resting on that layer, can be represented in Fig. 25 by the distance from the curve $W(t)$ to the straight line marked t'-layer; in this sense $w(t,t')$ may be called "weight-depth". Therefore the value of the integral $Q(t,t')$ expressed by formula (12) is represented by the area lying between the straight line of t'-layer and curve $W(t)$ in Fig. 25. Then the value of density $\rho(t,t')$ of t'-layer can be computed from equation (11) by using the numerical table of logarithmic integral (*8*). The relations between $Q(t,t')$ and ρ represented by equation (11) are graphed in the left half of Fig. 26 (next section) by three curves **a**, **b**, **c** each of which correspond to curves **a**, **b**, **c** of Fig. 24 respectively. On making those graphs the authors assumed the initial density ρ_0 to be 0.07 gr/cm^3, which value is generally observed on the newly fallen snow in the authors' district.

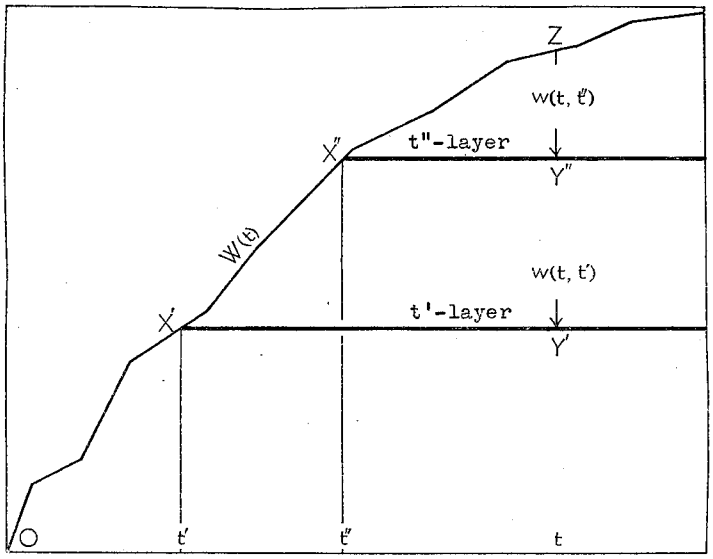

Fig. 25 Schema of accumulation of snow cover. $W(t)$ is the total weight of snow accumulated up to time t per horizontal unit area. The thick horizontal lines marked t'-layer and t''-layer represent respectively snow layers formed at time t' and t''; $w(t, t')$ and $w(t, t'')$ are the weight-depths, the weights of snow masses lying above the respective snow layers at time t.

Once the accumulation curve of snow cover is given, the value of $Q(t, t')$ at any time t is fixed by the distance ZY′ shown in Fig 25, that is, by the value of $w(t, t')$ at that time. If t''-layer which was formed at $t=t''$ is taken under consideration, the value of $Q(t, t'')$ concerning that layer at time t will be fixed by the distance ZY″, that is, by the value $w(t, t'')$. In this way distribution of density ρ within the snow cover at time t is, by the above described method, given at first as a function of the weight-depth w. In order to express the distribution of density in relation to the actual depth z from the snow surface use is made of the following relation

$$dw/dz = \rho(w), \tag{13}$$

which yields by integration a relation $z = \int_0^w dw/\rho(w) = F(w)$ to be used for converting $\rho(w)$ to $\rho(z)$. The total depth H of the snow cover at time t is given by

$$H(t) = F(w(t, 0)) = F(W(t)), \tag{14}$$

where $w(t, 0)$ is the weight-depth of the lowest layer of the snow cover at time t; it is the same thing as the total weight $W(t)$ of snow resting upon unit area of ground.

§ 23. Actual method employed for computing the density distribution within the snow cover.

If the actual computation were to be performed by the method described in the previous section tedious work would be required to determine $Q(t, t')$ for many different values of t and t'. Therefore the present authors simplified the computation by presuming that the actual way of accumulation of snow can approximately be replaced by the addition of a constant amount w_1 of snow to the snow cover every day. If such a presumption is granted, a straight line

$$W(t) = w_1 t \tag{15}$$

rising from the origin 0 towards the upper right can be substituted for the actual accumulation curve $W(t)$ of snow cover such as shown in Fig. 25. Then the value of $Q(t, t')$ comes to be represented by

$$Q(t, t') = \frac{1}{2}(t-t')\, w(t, t')$$

$$= \frac{1}{2} w_1 \cdot (t-t')^2 \tag{16}$$

$$= \frac{1}{2} w^2(t, t')/w_1 \tag{16'}$$

since $w(t, t') = w_1 \cdot (t-t')$.

In the right half of Fig. 26 is graphed relation (16) which exists between $Q(t, t')$ and $(t-t')$ for different values of w_1. Then one can determine the value of density ρ which the t'-layer takes on the day t by using the two groups of graphs shown side by side in Fig. 26. (Of the graphs shown in the left half of Fig. 26 an account was given in the previous section). For example, let the average rate w_1 of accumulation of snow cover be 0.7 gr/cm^2·day, the average temperature of t'-layer be -7°C and let the density ρ of that snow layer two weeks after its formation be required. One starts from point A, ascertains the 14-day point on the day-axis of the right figure of Fig. 26, and rises upright until he reaches the straight line marked point B. Then he goes towards the left to meet curve **a** at point C. Curve **a** should be chosen since this is the curve which corresponds to the temperature -7°C. Then he goes down and on the ρ-axis of the left figure finds point D. The value 0.243 indicated by point D is the required density of t'-layer.

By determining the value of ρ in the above described way for many snow layers corresponding to different values of t', that is, formed by precipitations of snow occurring on different days, ρ can be put in relation with w through the whole depth of the snow cover. Some examples of observed relations between ρ and w and the calculated one between them are graphed in Fig. 27. The observations were made on different days on one and the same snow cover which was continuing to accumulate on the flat ground near the authors' Institute in winter 1956–57; the dates attached to the observed curve indicate the dates of observation.

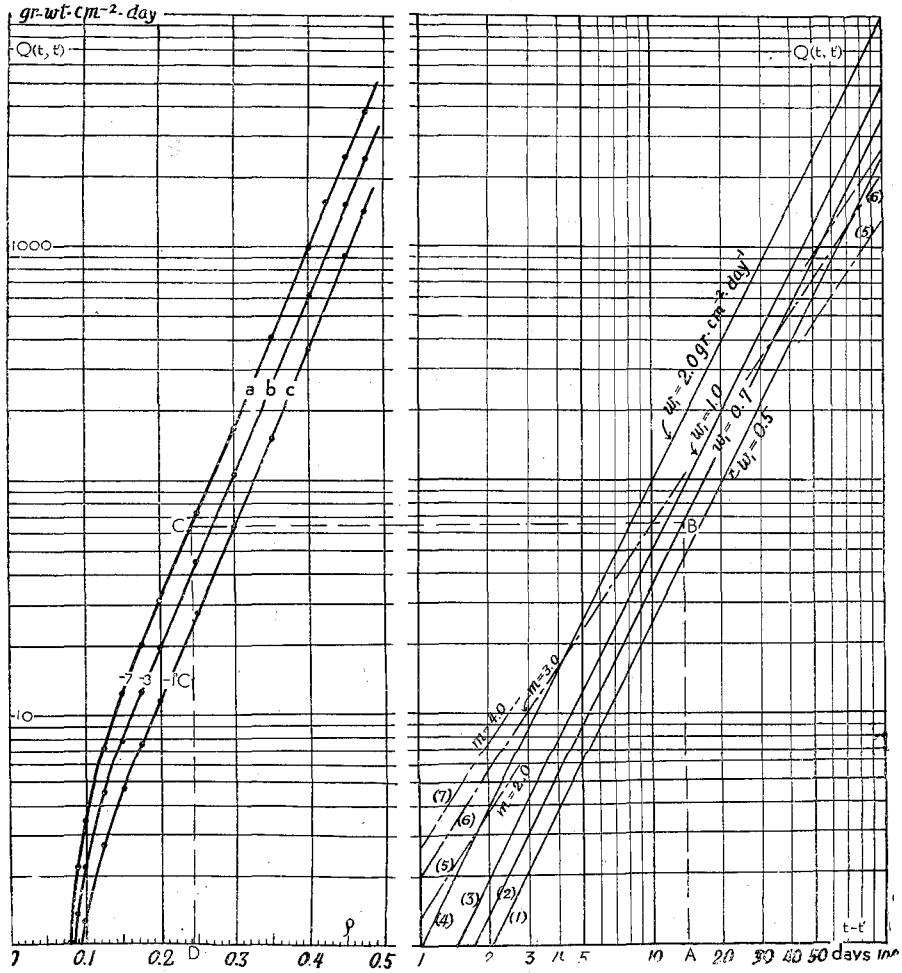

Fig. 26 Left: Relation between $Q(t,t')$ and the density ρ of snow. $Q(t,t')$ is the integrated action of the weight to which t'-layer has been subjected from the time of its formation to time t; it is equal to the area enclosed by X′ Y′ Y″ Z X″ X′ in **Fig. 25**. The relation is represented by three lines marked **a, b, c** computed from formula (11) in the text, that is, from $\eta_0\{\overline{Ei}(k\rho)-\overline{Ei}(k\rho_0)\}=Q(t,t')$ by putting $\eta_0=1.6$, 1.0, 0.6 gr-wt·day/cm² respectively and $\rho_0=0.07$ gr/cm³, $k=21.0$ cm³/gr common to the three. Each curve here corresponds respectively to each of the curves of Fig. 24 marked by the same letter.
Right: Relation between time $(t-t')$ and $Q(t,t')$ which is computed by assuming simple formulae such as $w_1\cdot(t-t')$ or $m\sqrt{t-t'}$ for the weight-depth $w(t,t')$.

The density ρ and the thickness h were measured on each of the snow layers composing the snow cover and the value of w at any level within the snow cover was obtained by summing up the product ρh for all the snow layers lying above that level. The computation on the basis of which the thick curve was drawn

was conducted by the aid of straight line $w_1=0.7$ and curve **b** of Fig. 26. Curve **b** was used since the average temperature of the snow cover was estimated to lie in the vicinity of —3°C. If the value of w_1 were chosen larger or smaller than 0.7 the calculated curve would have laid respectively below or above the one shown in Fig. 27. At first the observed curve laid below the calculated one (Dec. 20). Then it tended to be shifted upwards as time went on and came to coincide almost perfectly with the calculated one on Jan. 4. In actual fact the snow cover was increasing at the average rate 0.7 gr/cm²·day during the first decade of January. After that the observed curve moved upwards with actual decrease which occurred in the precipitation rate w_1, taking on Jan. 17 the position as shown in Fig. 27.

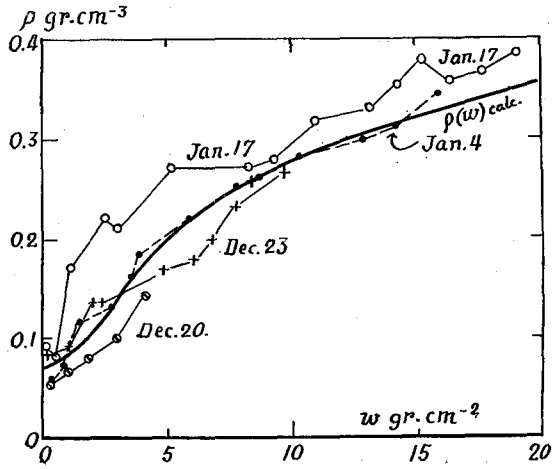

Fig. 27 Relation between the density ρ and the weight-depth w concerning one and the same snow cover observed on different days while the snow cover continued to be accumulated on the ground near the authors' Institute (Sapporo). The thick curve shows the relation computed by putting $W(t)=0.7\,t$.

The depth of snow cover on the ground at the authors' Institute exceeds seldom one meter. In order to test their method on much thicker snow cover the authors made a brief trip to the village "Mosiri" located in an experimental plantation belonging to Hokkaido University. Snow is deposited there to a depth greater than two meters every year and ordinary meteorological observations, including the observation of the depth of snow cover, are conducted as routine work.

The snow cover at Mosiri was investigated on Feb. 20, 1957, one hundred days after the first appearance of continuous snow cover at that place. The observed density ρ is plotted by small light circles against the observed w in the upper part (**a**) of Fig. 28. The total amount of snow precipitated during the preceding one hundred days which was obtained by summing up the precipitation data of the meteorological observation turned out to be 71 gr/cm² on the day of investi-

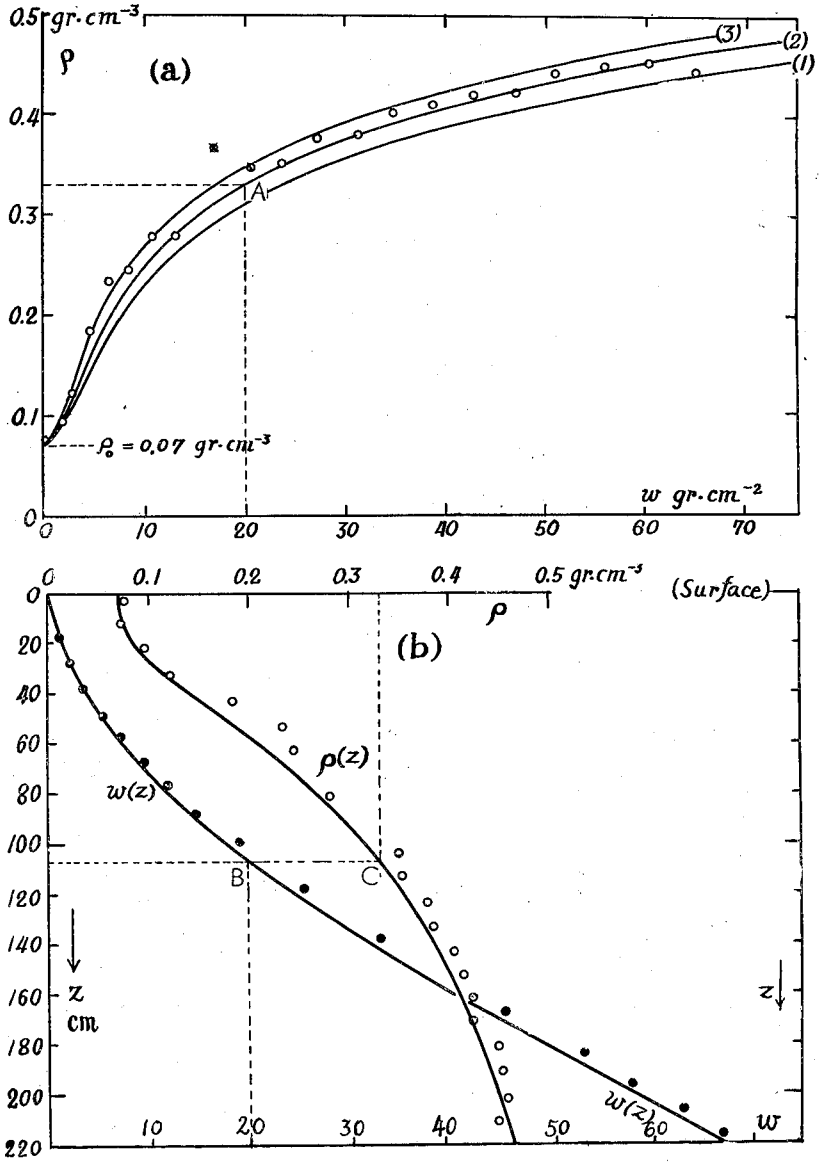

Fig. 28 Comparison of the results of computation with those of observation made on the snow cover at Mosiri.

Top, (a): the density ρ versus the weight-depth w. Light circles show the observed values. Two circles halved and quartered located near point A belong to layers of granular snow which occurred within the snow cover. Except those layers the snow cover was wholly composed of compact snow. The curves marked (1), (2), (3) are those computed by assumming $W(t)=1.0t$, $0.7t$, $0{,}5t$ respectively.

Bottom, (b): the vertical distribution $\rho(z)$ of the density expressed against the actual depth z from the surface of snow cover. The computed curve $\rho(z)$ was obtained from curve (2) of the top figure (a) by way of the curve $w(z)$ in this bottom figure. The observed points of ρ, light circles, lie rather close to the computed curve.

gation. Therefore the average rate w_1 of accumulation is found to have been 0.71 gr/cm²·day. The middle, marked (2), of three curves shown in Fig. 28 (**a**) was drawn by the aid of straight line $w_1=0.7$ and curve **a** of Fig. 26. Advantage was taken of curve **a** which corresponds to the temperature −7°C since the snow cover at Mosiri was estimated to have that temperature on the average judging from the mean temperature of air at that place. Curves (1) and (3) of Fig. 28 (**a**) are obtained by assuming $w_1=1.0$ and 0.5 gr/cm²·day respectively. As a whole, the light circles stand nearest to the middle curve (2) which was drawn by putting $w_1=0.7$ so as to agree with the actual average rate of accumulation of snow.

Now that a good agreement has been found between the observed and calculated relations between ρ and w, let the vertical distribution of snow density actually observed in relation to the depth z from the surface of snow cover be compared with the results of calculation. As was already mentioned at the end of §22, z is related to w by

$$z=\int_0^w \frac{dw}{\rho(w)}\ ; \tag{17}$$

z corresponding to any value w' of w is determined by measuring, say by using a planimeter, the area bounded by the w-axis, the vertical straight line $w=w'$ and a curve (not shown in the figure) representing $1/\rho(w)$ which can be derived from curve (2) of Fig. 28 (**a**). The curve marked $w(z)$ in Fig. 28 (**b**) was drawn on the basis of such a determination of z. The solid circles representing the observed values stand close to that curve. The distribution of the density ρ in dependence on z can be obtained by using that curve in combination with curve (2) of Fig. (**a**). Let two points corresponding to any same value of w, for example 20 gr/cm², be taken on the w-axes of the figures (**a**) and (**b**) of Fig. 28. The value of ρ corresponding to this value of w is determined as 0.33 gr/cm³ by crossing point A of curve (2) with the upright line through point 20 on the w-axis of figure (**a**). Then point C in figure (**b**) positioned at the distance 0.33 from the left edge of the figure on the horizontal line through point B, the cross point of curve $w(z)$ with the upright line standing upon point 20 of the w-axis of figure (**b**), turns out to be a point relating the density ρ with the depth z from the surface of snow cover. By applying such a procedure to different values of w one can obtain the curve $\rho(z)$ connecting ρ and z through the whole depth of snow cover as shown in figure (**b**). The light circles representing the observed value of ρ lie a little off to the right of that curve. But it may be said that the agreement between the observation and the calculation is rather good.

§24. Actual method employed for computing the total depth $H(t)$ of snow cover.

So long as the assumption noted in the previous section that the accumulation of snow cover can be represented by $W(t)=w_1 t$ is granted, the total depth $H(t)$ of

the snow cover any number t of days after the first appearance of continuous snow cover on the ground can be obtained by a computation which is simpler than that explained at the end of §22. The simplicity of computation depends upon such a situation that all the snow layers composing the snow cover should alter in density according to the same formula depending only on the time interval $(t-t')$ elapsed since their formation, regardless of the time point t' when they are formed.

Indeed three formulae (11), (12) and (16) shown in the previous section yield

$$\eta_0\left\{\overline{Ei}\,(k\rho)-\overline{Ei}\,(k\rho_0)\right\}=(t-t')^2\cdot w_1/2\,, \tag{18}$$

which gives the density $\rho(t,t')$ of t'-layer at time t as a function of $(t-t')$. Now let r denote any variable and let that function be represented by $f(r)$ when expressed in dependence on that variable. ($f(r)$ is the same function as $\rho(t-t')$ in which r is substituted for $t-t'$.) If $f(r)$ is graphed it appears as the curve marked $f(r)$ shown in Fig. 29.

If t'-layer is considered to have been formed during a short time interval from t' to $t'+dt'$, it contains within itself the mass of snow equal in amount to w_1dt' per horizontal unit area. Therefore it comes to contribute to the depth of snow cover at time t by a small thickness $dz=w_1dt'/\rho(t,t')$. Then, since the total depth $H(t)$ of snow cover at time t should be equal to the sum of the contributions from all the t'-layers which have been formed before that time, $H(t)$ is given by

$$H(t)=\int dz=\int_0^t\frac{w_1dt'}{\rho(t,t')}=\int_0^t\frac{w_1dt'}{\rho(t-t')}=\int_0^t\frac{w_1dr}{f(r)}\,. \tag{19}$$

The integrand of the last integral is shown in Fig. 29 by the curve marked $w_1/f(r)$; the value of $H(t)$ can be determined by applying the method of quadrature to this curve.

In Fig. 29 are shown two curves of $H(t)$ obtained in the above way for two values 0.7 and 1.0 of w_1. The small light circles show the depths of snow cover observed by the meteorological observatory of Mosiri. They agree with the $H(t)$-curve with $w_1=1.0$ during the first period of about 50 days, but thereafter begin to leave that curve to draw near the $H(t)$-curve with $w_1=0.7$ coming to lie very close to the latter curve after the 80th day. Such a passage of the observed points (small light circles) from one of the $H(t)$-curves to another with different value of w_1 was caused by the change in the rate of accumulation w_1 which occurred actually to the snow cover of Mosiri. The small solid circles in Fig. 29 show the integrated amounts W of precipitated snow which were determined by adding the daily amounts of precipitation registered by the pulviometer. They are located along $W(t)$-line with $w_1=1.0$ as long as the light circles lie near $H(t)$-curve with $w_1=1.0$. Then they move towards $W(t)$-line with $w_1=0.7$ in step with the light circles passing from $H(t)$-curve with $w_1=1.0$ to that with $w_1=0.7$.

But the above noted good agreement in the later stage of observed values of

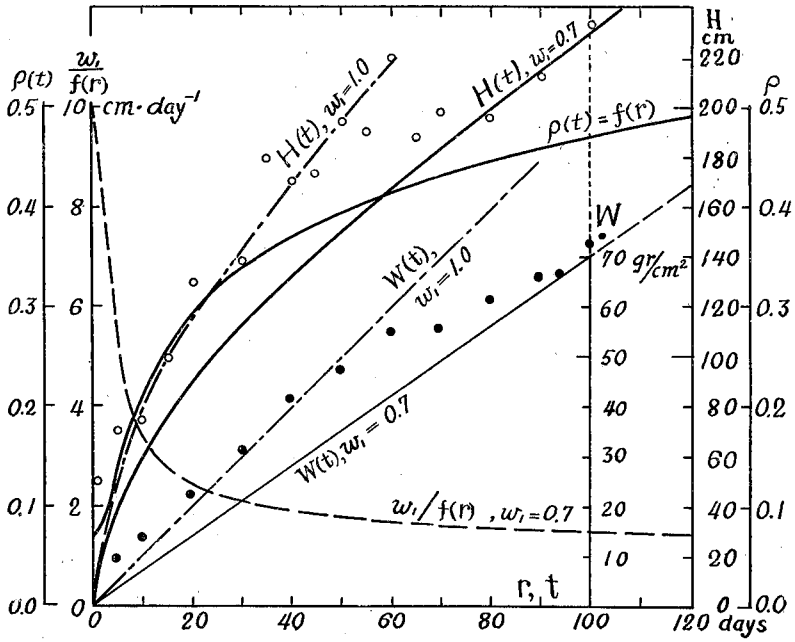

Fig. 29 The curves marked $H(t)$ show the computed depth of snow cover in dependence on time t counted from the first appearance of continuous snow cover. They were obtained on the assumption that the snow was accumulated according to $W(t)=w_1 t$ with the values of w_1 attached to them. The depth observed on the actual snow cover at Mosiri is represented by light circles; they lie near curve $H(t)$, $w_1=1.0$ for the first period of about 50 days and thereafter tend to be positioned near curve $H(t)$, $w_1=0.7$. The solid circles show the accumulation of snow at Mosiri obtained by adding the daily precipitation recorded by a pulviometer. They stand along curve $W(t)$, $w_1=1.0$ up to about 50th day but then are displaced towards curve $W(t)$, $w_1=0.7$.
$f(r)$ is a function giving the density ρ which a snow layer takes r days after its formation. Curves $H(t)$ can be obtained by applying the method of quadrature to the curve of $w_1/f(r)$.

snow depth with the calculated ones must rather be thought of as a wrong result because such an agreement should occur only when the snow cover continued from the very first to increase at the unchangeable rate $w_1=0.7$. It should have been expected that the observed points would depart downwards from the $H(t)$-curve with $w_1=1.0$ about the time of the 50th day but not to approach so close to that with $w_1=0.7$ as seen in Fig. 29. The authors suppose that some causes other than the shrinkage of snow layers such as slow melting of the snow cover at its bottom also exerted effect in reducing its thickness.

§ 25. Remarks.

(*1*) Anyone who has once practised the measurement of snow precipitation

by a pulviometer knows well that the instrument catches the falling snow only below the amount which it should do. Wind carries the light snow crystals and flakes away from the mouth of the instrument. Then the good agreement between the observed and computed results described in the previous sections will be thought of as a wonder because the computations were executed on the basis of the data of precipitation obtained by the pulviometer. On that point the authors made the following examination. They fixed on each of the snow layers composing the snow cover at Mosiri the date of its formation by comparing the stratification of the snow cover with the register of the snow falls in the past. The amount of fallen snow registered by the pulviometer for any snow fall was then found to be the same as that contained in the snow layer which was formed by that snow fall. Therefore the pulviometer at Mosiri had registered the correct value of snow precipitation. It was fortunate that the wind was weak through the winter at Mosiri as was confirmed by the meteorological record of wind velocity.

(2) Although the assumption $W(t)=w_1 t$ for the accumulation curve makes the computation simple, there may arise cases where such an assumption is in too great deviation from actuality. When the accumulation curve is different from the linear form $W(t)=w_1 t$, the mode of change in density ρ differs from one snow layer to another according to the time point t' when the snow layer is formed. As an example, let a case where $W(t)$ is represented by $m\sqrt{t}$ be considered. Then the weight-depth $w(t,t')$ for t'-layer is given by $m(\sqrt{t}-\sqrt{t'})$ and the integral $Q(t,t')=\int_{t'}^{t} w(t,t')\,dt$ comes out to be

$$\begin{aligned} Q(t,t') &= \int_{t'}^{t} m(\sqrt{t}-\sqrt{t'})\,dt \\ &= (2/3)\,m(\sqrt{t^3}-\sqrt{t'^3})-m(t-t')\sqrt{t'}\ , \end{aligned} \tag{20}$$

which depends not only on the time interval $(t-t')$ elapsed since the formation of t'-layer but also on the time point t' when it was formed. The density ρ, being such a quantity as to be determined by equation (11) which contains $Q(t,t')$, must also depend on $(t-t')$ as well as on t'. In the case of linear accumulation, $w(t,t')$ being equal to $w_1\cdot(t-t')$, $Q(t,t')$ depends only on $(t-t')$ but not on t' itself. On account of such a situation the computations of total depth $H(t)$ of snow cover or density distribution $\rho(z)$ within it must become more complicated in the cases different from the linear case $W(t)=w_1 t$.

In the following some considerations will be presented on the manner of change in density ρ caused to a snow layer by weight-depth $w(t,t')$ which changes with time in a way different from $w_1(t-t')$. (It should be noticed that attention is paid here only to a single snow layer which is subjected to a special load. It does not concern things about a snow cover composed of many snow layers). In figure (**a**) of Fig. 30 are shown four simple curves for $w(t,t')$ including that for $w_1\cdot(t-t')$. The respective mathematical formulae corresponding to them are shown in the

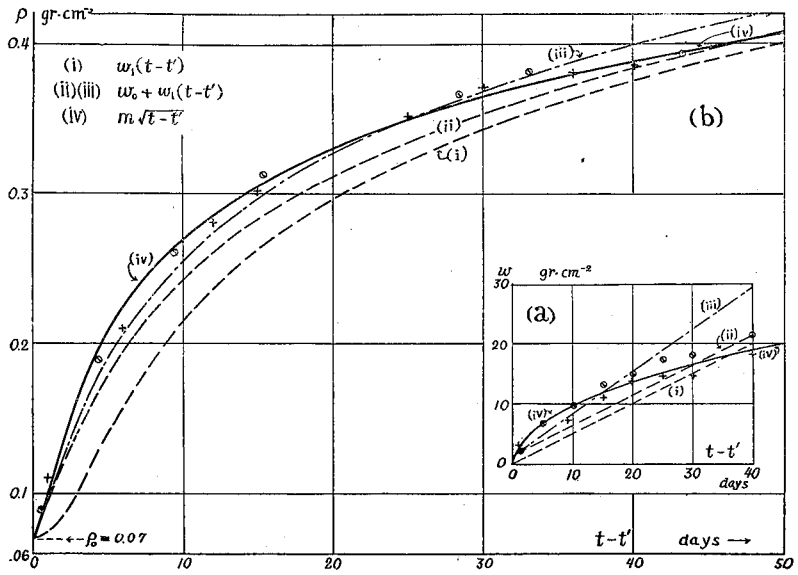

Fig. 30 (a) Simple curves useful for approximating the actual weight-depth $w(t, t')$; the mathematical formulae for them are found in the upper left corner of part (b).
(b) Density ρ which a snow layer will take under the action of $w(t, t')$ is plotted against time $t-t'$.
The halved circles and crosses represent the values observed on certain two snow layers; they lie closest to curve (iv) in both portions (a) and (b).

upper left corner of figure (**b**). According to the authors' experience $w(t, t')$ for any actual snow layer seems to be approximated by some of the formulae presented here. The four curves in figure (**b**) indicate respectively the density ρ of snow layers which are subjected to the load $w(t, t')$ shown by the curves in figure (**a**). The values of density ρ were determined in a way similar to that explained in the previous sections. For example, the values for case (iv) were obtained as follows. In the right half of Fig. 26, $Q(t, t')=\int m\sqrt{t-t'}\,dt$ is graphed against $(t-t')$ by chain lines for different values of m. By using one of those lines in combination with one of the curves in the left half of the figure, the density ρ which a snow layer will take on any day after it has begun to be loaded with weight $m\sqrt{t-t'}$ can be determined just in the same way as explained in § 23. From Fig. 30 one will see what an influence the difference in $w(t, t')$ acting upon a snow layer has on its density.

The crosses and halved circles in Fig. 30 represent values of $w(t, t')$ and ρ actually observed on a certain two snow layers. They lie near to the curves marked (iv) in both (**a**) and (**b**) of Fig. 30.

(3) A snow layer deposited at one snow-fall shrinks, until the next snow-fall occurs, exclusively due to its own weight with no snow layer resting upon it. For

the sake of convenience for making numerical computations on the shrinkage in that interval, let the snow layer be assumed to have uniform density ρ_0 through its whole thickness at the end of the snow-fall, and let time t be counted from that instant. When the snow layer is thought of as being composed of a great number of thin snow sheets, the weight w acting upon any one snow sheet is, of course, larger as that sheet lies deeper in the snow layer. But w remains unaltered for any one and the same sheet in spite of the shrinkage of the snow layer and any one of the sheets can be distinguished from others by naming it by the value of w proper to it.

The density ρ of the sheet designated by w is given by

$$\eta_0 \int_{\rho_0}^{\rho} \exp(k\rho)\, d\rho/\rho = \eta_0 \left\{ \overline{Ei}(k\rho) - \overline{Ei}(k\rho_0) \right\} = wt\,, \tag{21}$$

since $Q(t, t')$ turns out to be $\int w dt = wt$ in this case (cf. equations (9), (11), (12) of §22). The curves in the right half (**a**) of the upper part of Fig. 31 show, for different values of t, the relations between ρ and w obtained by means of equation (21).

Let the distance taken downwards from the top of the snow layer be denoted by z. Then the differentiation of the above equation with respect to z gives

$$\eta_0 \left\{ \exp(k\rho)/\rho \right\} (d\rho/dz) = t\,(dw/dz)\,,$$

which can be rewritten in the form

$$\eta_0 \left\{ \exp(k\rho)/\rho^2 \right\} d\rho = t\, dz\,, \tag{22}$$

since $dw/dz = \rho$ (cf. equation (13) of §22). Then by the integration of this equation one gets the relation

$$k \left\{ \overline{Ei}(k\rho) - \overline{Ei}(k\rho_0) \right\} - \left\{ \exp(k\rho)/\rho - \exp(k\rho_0)/\rho_0 \right\} = (t/\eta_0) z\,, \tag{23}$$

which yields ρ as a function of z and t. The group of curves in the left half (**b**) of the top portion of Fig. 31 represents the density distribution $\rho(z)$ for different values of t computed by means of equation (23) under the assumption that $k = 20.2$ cm^3/gr, $\rho_0 = 0.07$ gr/cm^3 and $\eta_0 = 1.00$ gr-wt·day/cm^2.

If the distance taken at $t = 0$ downwards from the top of the snow layer is denoted by z_0, there holds the relation $w = \rho_0 z_0$; the top edge of Fig. 31 (**a**) is graduated by z_0. Then it can be known from the two parts (**a**) and (**b**) in combination how far the snow sheet located at depth z_0 at $t = 0$ will be below the top surface of the snow layer at any later time t. As an example let the snow sheet located at $z_0 = 50$ cm be taken under consideration. Draw a line downwards from point $z_0 = 50$ cm on the top edge of part (**a**) and extend horizontal lines towards the left from each of the crossing points A, B, C, etc. of that vertical line with the curves of (**a**). The horizontal lines meet respectively at points A′, B′, C′, etc. the curves

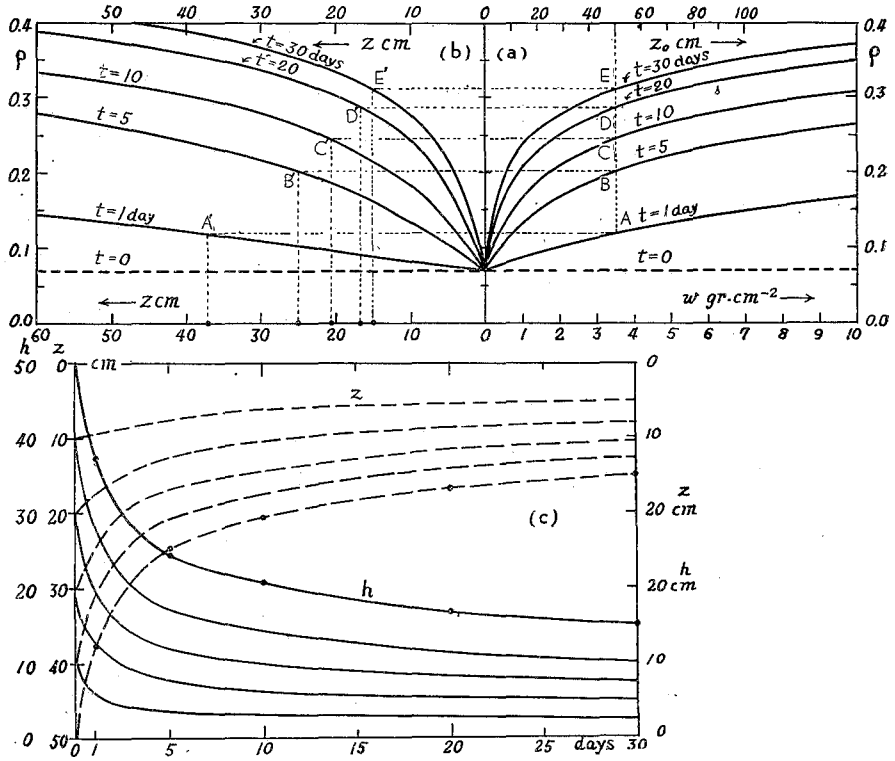

Fig. 31 Shrinkage of a snow layer during the interval from the time of its formation to the time of occurrence of the next snow-fall. The surface sub-layers of initial thickness z_0 will be diminished in their thickness z as indicated by the distances from the top edge of part (c) to the broken-line curves. If the snow layer deposited on the ground is initially 50 cm thick, its top will sink as time goes on as shown by the uppermost of the thick curves of part (c). The thick-line curves were constructed by shifting the broken curves downwards, keeping the vertical distances between them unaltered, until the lowest of them became coincident with the bottom edge of part (c).

in part (**b**) attached with the same values of t as those of part (**a**) from which they have started. The feet of the upright lines standing on the bottom edge of part (**b**) and passing through points A′, B′, C′, etc. give the values of z which the snow sheet in question will take at the respective time t. In the present case of $z_0=50$ cm, the sheet takes $z=37.0$, 24.4, 20.6, 16.7, 15.0 cm for $t=$ 1, 5, 10, 20, 30 days respectively. The values of z determined in this way for $z_0=$ 10, 20, 30, 40, 50 cm are represented in the bottom portion (**c**) of Fig. 31 by the distances from its top edge to the broken curves. If the snow layer is deposited on the ground and its initial thickness is 50 cm, the position of its top surface will descend as time goes on in such a manner as represented by the uppermost of the five thick curves shown in part

(c) of Fig. 31. The group of thick-line curves is constructed by shifting downwards the whole group of the broken curves so as to make the lowest curve of the latter group coincide with the bottom edge of the figure. If the initial thickness is 30 cm, the downward shift should be so made that the broken line belonging to $z_0=30\,\mathrm{cm}$ would coincide with the bottom edge.

(4) As was described in § 21, when compact snow is made to become granular in structure by partial thawing or by formation of depth hoars, the coefficient of viscosity η rises very rapidly with increasing density ρ as indicated by the upward bends of $\log\eta$—ρ curves shown in Fig. 24. In such cases the relation between η and ρ can often be represented by

$$\eta=\eta_0\left(\frac{\rho_\infty-\rho}{\rho_\infty}\right)^{-b}, \tag{24}$$

where b and η_0 are a positive constant and the coefficient of viscosity for $\rho=0$

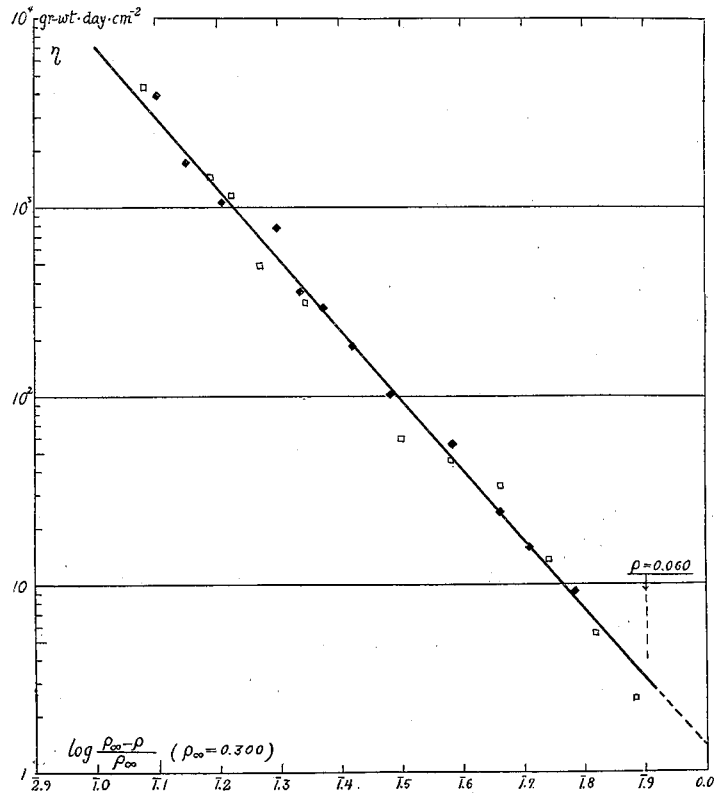

Fig. 32 When snow in the snow cover changes from compact snow into granular type the relation between the coefficient of viscosity η and the density ρ is often found to be represented by $\eta=\eta_0\left(\frac{\rho_\infty-\rho}{\rho_\infty}\right)^{-b}$.

respectively while ρ_∞ means the density for $t=\infty$. Two examples of snow layers which changed in η according to this formula on account of the formation of depth hoars within them are shown in Fig. 32. The marks representing the observed values of η are located close to the straight line which shows the above formula in the altered form of

$$\log \eta = \log \eta_0 - b \log \left(\frac{\rho_\infty - \rho}{\rho_\infty} \right) . \tag{25}$$

It is needless to say that the method of computation described in § 22 is applicable with no other alteration than substituting formula (24) for formula (7) of § 21 if it is necessary to deal with snow layers changing into granular snow.

Summary

The Contraction of Snow at Constant Speeds. §§**15–20.**

Snow shrinks with no sign of fracture when compressed very slowly as in the case of the contraction of snow cover in nature by its own weight. On the other hand, snow suffers a destructive contraction if it is forced to contract quickly as when it is trod upon by foot. In this way the manner of contraction of snow differs essentially according to whether it is compressed slowly or quickly; the manner of contraction must stand in a close relationship with the speed of contraction. In order actually to see such a relationship a pillar of snow was compressed at different constant speeds and the force with which the snow resisted the compression was registered by a recording galvanometer or by an electromagnetic oscillograph. The speed of compression was varied from 1 mm/min to 1 m/min. At speeds of ten to twenty mm/min the curve of resisting force took the form of saw-teeth; the resistance R, starting from the minimum value R_*, rose to reach the maximum R^*, and then suddenly dropped to R_* to begin at once to rise again towards R^*. As long as the compression lasted R continued to repeat such a variation. The pillar of snow was lessened in height by being broken into fragments of ice near its top or bottom plane, without the remaining portion undergoing any contraction. Let such a type of compression be called "destructive contraction".

As the speed of compression was decreased the saw-teeth of the curve of resistance became broader, and finally no drop from R^* to R_* made an appearance when the time of experiment was a few minutes. In this case resistance R rose rather rapidly up to a certain value at first after which rise it began to continue increasing at a small constant speed until the end of the experiment. The pillar of snow ceased to break at the end plane and contracted uniformly through its whole height. Let the compression of this sort be called the "plastic type."

Also, when a thick metal plate was forced into a large block of snow at different speeds, the reistance to the plate changed with the speed just as in the above case of a snow pillar. The two types, destructive and plastic, could be distinguished in

the contraction occurring to the snow located below the plate. In the case of destructive contraction a distinctly bounded region of compressed snow developed immediately below the plate. The fragments of ice into which the end of snow pillar broke must have accumulated to form that region in this case. When the block of snow was compressed so slowly as to undergo plastic compression no region of compressed snow appeared.

When the compression speed was increased instead of being decreased, the saw-teeth of the curve of resistance R became narrow, the drop from R^* to R_* becoming small at the same time. Finally the saw-tooth character disappeared and R came to show a continuous curve with small fluctuation. At the same time the fragments of ice into which the end plane of the snow pillar had been breaking came to unite themselves to form a thin plate hanging from the end of the pillar like a tongue. Let the compression occurring in this way be called "destructive contraction of the second kind."

The critical speeds which divided the destructive contraction from the plastic one as well as from the destructive one of the second kind both depended on the temperature. The former critical speed decreased while the latter one increased as the temperature was lowered.

Independently of the above noted types of contraction a decrease in the resistance R accompanied the increase of compression speed. On the basis of this fact some discussion was offered on the mechanism of the occurrence of an avalanche. It is a general rule that an advancing phenomenon develops to an outbreak if the increase of its speed of advance is accompanied by the diminution of resistance.

Numerical Computation of the Thickness of Snow Cover from the Amount of Precipitated Snow. §§ 21–25.

The snow layers composing snow cover on the ground shrink as time goes on and their compressive viscosity η is increased as their density ρ is enlarged due to the shrinkage. By making observations on a number of snow layers, the present authors had, as reported in Part II of this series of papers, found a simple relationship

$$\eta = \eta_0 \exp(k\rho)$$

to exist between η and ρ. The total snow depth H at any time t after the commencement of snow season could be computed by the use of that formula from the precipitation data of snow up to that time in good accordance with the actual total depth of snow cover. (Here symbol H is used for convenience of mathematical description in place of HS which is the symbol to be used for the total snow depth after the International Classification of Snow.) The distribution of computed density within the snow cover also agreed well with that of the density which was actually

observed. It is hoped that the reverse procedure, that is, the computation of water equivalent *HW* of snow cover from *HS* which is of great practical importance, will in the future be accomplished by further advance on such a course of study.

References

"T. K." in the following is the abbreviation for "Teion-Kagaku" (Low Temperature Science), a scientific publication written in Japanese, issued by the Institute of Low Temperature Science, Hokkaido University, Sapporo, Japan.

(1) Seiiti KINOSITA 1957 The relation between the deformation velocity of snow and two types of its deformation (plastic and destructive). T. K. (Physics) **16**, 139-166.

(2) Iwao FURUKAWA and Yoshimi SHIRAI 1948 Resistance of snow against a slow compression (in Japanese). Journ. of Japanese Soc. of Snow and Ice. **10**, 128-132.

(3) R. SAITO 1949 Physics of fallen snow. Geophysical Magazine (Tokyo) **19**, 1-56.

(4) J. K. LANDAUER 1955 Stress-strain relations in snow under uniaxial compression. Research Paper, **12**, S.I.P.R.E.

(5) Lorne W. GOLD 1956 The strength of snow in compression. Journal of Glaciology, **2**, 719-725.

(6) Edwin BUCHER Beitrag zu den theoretischen Grundlagen des Lawinenverbaus. Beiträge 2, Geol. Schweiz. Hydro., Lief. 6.

(7) Kenji KOJIMA 1957 Viscous compression of natural snow layers. III. T. K. (Physics) **16**, 167-196.

(8) K. A. KARPOV and S. N. RAZUMOVSKY 1956 Tablitsy integralinogo logarifma. Akademiya Nauk SSSR.